Influence of plant growth form, habitat and season on leaf-wax n-alkane hydrogen-isotopic signatures in equatorial East Africa

Journal Article

Author(s):
Griepentrog, Marco ; De Wispelaere, Lien; Bauters, Marijn; Bodé, Samuel; Hemp, Andreas; Verschuren, Dirk; Boeckx, Pascal

1 # Influence of plant growth form, habitat and season on leaf-wax
2 # *n*-alkane hydrogen-isotopic signatures in equatorial East Africa

3 **Marco Griepentrog [a,b,c,*], Lien De Wispelaere [a], Marijn Bauters [a,d], Samuel Bodé [a]**
4 **Andreas Hemp [e], Dirk Verschuren [f,1], Pascal Boeckx [a,1]**

5 [a] Isotope Bioscience Laboratory (ISOFYS), Department of Green Chemistry and Technology, Ghent
6 University, Ghent, Belgium

7 [b] Biogeoscience, Department of Earth Science, ETH Zurich, Zurich, Switzerland

8 [c] Soil Resources, Department of Environmental Systems Science, ETH Zurich, Zurich, Switzerland

9 [d] Computational and Applied Vegetation Ecology (CAVE) Lab, Department of Environment, Ghent
10 University, Ghent, Belgium

11 [e] Department of Plant Systematics, University of Bayreuth, Bayreuth, Germany

12 [f] Limnology Unit, Department of Biology, Ghent University, Ghent, Belgium

13

14 [*] Corresponding author
15 E-mail address: marco.griepentrog@usys.ethz.ch
16 Phone: +41 44 63 36079

17 [1] Equal contribution

Abstract

   Leaf-wax n-alkanes are produced by terrestrial plants, and through long-term preservation in sediments their stable hydrogen-isotopic signature (δ^2H_{wax}) provides useful information on past hydrological variation for paleoclimate reconstructions. However, gaps remain in our understanding of the relationships between the isotopic signatures of leaf waxes and the plants' source water. In this study, we investigated the influence of plant growth form, habitat and season on the distribution patterns and δ^2H_{wax} values of 14 plant species (among which are two grasses, five trees and seven shrubs) sampled during four successive dry and wet seasons in three distinct habitats around Lake Chala in equatorial East Africa. Variation in δ^2H_{wax} was analyzed with linear mixed-effect models and compared with the associated values of xylem water (δ^2H_{xylem}), leaf water (δ^2H_{leaf}) and biosynthetic hydrogen fractionation (ε_{bio}). Our results show that plant growth form was the most important driver of modern-day δ^2H_{wax} variability in the study area, and that differences in δ^2H_{wax} among habitats to a large extent reflect how each major growth forms is represented in those habitats. Individual plant species appear to express substantial species-specific isotopic fractionation that cannot be attributed to the tested external factors but rather seem to depend on intrinsic (e.g., plant phenological and biosynthesis-related) factors. For the purpose of calibrating δ^2H_{wax} signatures against vegetation types, it is thus crucial to analyze representative samples of the plant communities present in the study area. Our results further indicate that paleohydrological studies in regions receiving rain from multiple moisture sources must take into account possible seasonal bias in the δ^2H_{wax} signature relative to annual rainfall, due to unequal use of those moisture sources by the plants. Finally, the strong influence of plant growth form on δ^2H_{wax} values argues for δ^2H_{wax} variation in paleo-records being evaluated in conjunction with independent proxy data on changes in vegetation composition. Differences in n-alkane distribution patterns among trees, shrubs and grasses (e.g., average chain length, carbon preference index and $C_{31}/(C_{29}+C_{31})$ ratio) may provide such proxies, and can be produced from the same leaf-wax n-alkane dataset used to determine δ^2H_{wax}.

Keywords: Organic geochemistry; Paleohydrology; Hydrogen-isotopic fractionation; Lipid biomarker proxies; Plant physiology; Biosynthetic pathways; Hydrological cycle; Net enrichment; Leaf-wax n-alkanes; Moisture sources; Hydroclimate reconstruction

1. INTRODUCTION

Climate models developed to predict future climate change are continuously refined by our understanding of current and past climate variability. Particularly crucial in this regard are the temporal dynamics of tropical hydrological systems, as these strongly shape global climate (Schneider et al., 2014). In this context, paleoclimate research in the tropics provides important counterparts to the better-established records from polar and north-temperate regions (Clement et al., 2004). One widely used proxy in the reconstruction of past tropical climate variability are leaf-wax n-alkanes (δ^2H_{wax}) extracted from marine and lake sediments (e.g., Schefuß et al., 2005; Tierney et al., 2008; Tierney et al., 2011; Berke et al., 2012; Costa et al., 2014; Garcin et al., 2018). Hydrogen in leaf-wax n-alkanes originates from the plant's source water and as a result the δ^2H_{wax} values of terrestrial plants show a strong relationship with the hydrogen-isotopic signature of precipitation (e.g., Sachse et al., 2004; Polissar and Freeman, 2010; Garcin et al., 2012); see Sachse et al. (2012) for a general review of the method.

Spatial and temporal patterns in the isotopic signature of precipitation (δ^2H and $\delta^{18}O$) are affected by several environmental variables including temperature, relative humidity and origin of the precipitation water (Craig, 1961; Dansgaard, 1964; Gat, 1996). Consequently, δ^2H values of past precipitation as recorded in leaf-wax n-alkanes extracted from sedimentary archives may provide invaluable information on past hydrological variability. After litter fall or through atmospheric transport (Nelson et al., 2018), leaf waxes are temporarily stored in soils (Griepentrog et al., 2016), delivered to lakes (Feakins et al., 2018) and ultimately buried in sediments (Douglas et al., 2014), where they are relatively resistant to microbial breakdown (Schimmelmann et al., 1999) and can thus be preserved over long time scales, at least in suitable depositional systems (Eglinton and Eglinton, 2008). However, for correct interpretation of a sedimentary leaf-wax archive located in a particular region it is important to understand the region's modern-day hydrogen-isotopic 'signature transfer' system, which includes 1) the isotopic fractionation taking place during the incorporation of hydrogen from the plants' source water into their leaf waxes, and 2) the spatial and temporal integration of the hydrogen-isotopic signature which occurs until delivery of the waxes to the lake and their permanent burial in the lake-sediment archive. Focusing on the first issue, and despite the great potential of hydrogen-isotopic signatures of leaf waxes as a paleohydrological proxy, major uncertainties remain about the 'net' (or 'apparent') hydrogen-isotopic fractionation (ε_{net}) between plant source water and leaf-wax n-alkanes (Sachse et al., 2012).

Most plants do not capture precipitation directly but tap into soil water. The isotopic signature of plant source water is determined by the depth at which plant roots access this soil water, because the evaporation of soil water, which affects its isotopic composition, decreases with soil depth (Dawson and Ehleringer, 1991; Evaristo et al., 2015). The isotopic signature of xylem water is considered equal to that of the used soil water, as most commonly no isotopic fractionation is observed during water uptake and transport through the roots (White et al., 1985). However, recent research suggests that isotopic fractionation may nevertheless occur, at least in xerophytic species (Ellsworth and Williams, 2007) and under arid conditions (Zhao et al., 2016); and that it can be enhanced by the presence of arbuscular mycorrhizas (Poca et al., 2019).

Transpiration via the leaves to the ambient atmosphere results in further isotopic enrichment of leaf water compared to xylem water (Cernusak et al., 2016). Temperature and RH of the atmosphere, the isotopic signature of water vapor surrounding the plant, and leaf phenology (deciduous versus evergreen) in relation to seasonal variability in these atmospheric variables concurrently determine the relative

isotopic enrichment of leaf water (Kahmen et al., 2008; Kahmen et al., 2013). Finally, leaf water (or in the case of grasses, a mixture of xylem and leaf water) is the ultimate source of hydrogen for the biosynthesis of leaf-wax *n*-alkanes, which are usually strongly isotopically-depleted in hydrogen compared to leaf water, due to strong hydrogen-isotopic fractionation during biosynthesis (e.g., Sessions et al., 1999); the latter can be due to differences in metabolic pathways, hydrogen transfer reactions and extrinsic environmental factors (Eley et al., 2014; Newberry et al., 2015; Cormier et al., 2018).

The 'net' fractionation (ε_{net}) between plant source water and leaf-wax *n*-alkanes integrates three potential sources of isotopic fractionation: soil water evaporation, leaf-water transpiration and biosynthetic fractionation. Thus, constraining each of these three sources of variability is paramount for paleohydrological interpretation (Smith and Freeman, 2006; Liu and Yang, 2008; Sachse et al., 2012). Therefore, the spatiotemporal variation in δ^2H_{wax} (but also of source, xylem and leaf water) needs to be determined across the terrestrial ecosystems from which leaf waxes are transported into the studied sediment archive. In the present study, we report observations from a data-scarce tropical region in equatorial East Africa, with the overarching aim to improve mechanistic understanding required for reliable interpretation of δ^2H_{wax} as paleohydrological proxy. We investigated the distribution patterns (i.e. average chain length and carbon preference index) and δ^2H_{wax} from diverse species and growth forms of terrestrial plants in three distinct habitats around Lake Chala, during four successive wet and dry seasons between December 2013 and July 2014. This data is compared with δ^2H values from a wide range of water sources, including local precipitation as well as plant xylem and leaf water, to determine the hydrogen-isotopic fractionation between the distinct water sources and the leaf-wax *n*-alkanes. Furthermore, we evaluated the influence and relative importance of plant growth form, habitat and seasonality in order to answer the following questions:

1) How do leaf-wax *n*-alkane distribution patterns and their hydrogen-isotopic signatures (δ^2H_{wax}) vary across different plant growth forms, habitats and seasons?

2) Can δ^2H_{wax} values be explained by the hydrogen-isotopic signatures of plant xylem water (δ^2H_{xylem}), leaf water (δ^2H_{leaf}) or the biosynthetic hydrogen fractionation (ε_{bio}), and how do these vary across different plant growth forms, habitats and seasons?

3) What are the implications for paleohydrological studies, which apply the hydrogen-isotopic signature of leaf-wax *n*-alkanes (δ^2H_{wax}) to reconstruct past climate variability?

2. MATERIAL AND METHODS

2.1. Study site

Our study sites are located in three distinct plant habitats (crater rim, lakeshore and savanna) surrounding Lake Chala (3°19'S, 37°42'E; locally spelled 'Challa' after a nearby village), a 4.2 km², ca. 92-m deep crater lake (Moernaut et al., 2010) situated at 880 m above sea level (m a.s.l.) on the southeastern slope of Mt. Kilimanjaro in equatorial East Africa. This region has a pronounced bimodal rainfall seasonality, induced by bi-annual passage of the tropical rain belt across the equator (Nicholson, 2018). Southeasterly (SE) 'long' monsoon rains from March to May and northeasterly (NE) 'short' monsoon rains from late October until December are separated by a short dry season in January-February and a long dry season from June until mid-October (Nicholson, 2000). The local climate is tropical semi-arid with mean annual precipitation of ca. 530-650 mm and mean annual temperature of 25.5 ± 1.2°C

127 (mean ± 1σ; Hemp, 2006; De Wispelaere et al., 2017). As recorded at the town of Voi, ca. 80 km east of
128 Lake Chala, highest mean monthly day- and nighttime temperatures occur in February-March (ca. 33
129 and 21 °C, respectively) and lowest in July-August (ca. 28 and 18 °C, respectively; Buckles et al., 2014;
130 De Wispelaere et al., 2017). A detailed description of the vegetation at our three distinct sampling sites
131 can be found in Hemp (2006). In short, the vegetation of the crater basin and rim surrounding Lake Chala
132 consists of different types of open forest and savanna woodland with either succulent or deciduous
133 species dominating the tree layer. The lakeshore is rimmed by a narrow fringe of tropical evergreen
134 forest. The dominant vegetation on the outer crater slopes and in areas further afield is dry savanna
135 woodland with C_4 grasses.

136 **2.2. Sample collection**

137 Plant materials were collected during four successive seasons in 2013-2014: the short rain season
138 (December 2013, NE monsoon), the short dry season (February 2014), the long rain season (April 2014,
139 SE monsoon) and the long dry season (July 2014). However, because the 2014 long rain season atypically
140 started already in February, our data for the short dry season is likely influenced by SE monsoon rainfall.
141 In total, 14 locally common plant species representative for the region and including the three principal
142 growth forms (grass, shrub or tree; Table 1) were selected across three contrasting local habitats:
143 lakeshore forest, and savanna woodland with either shallow or deep soils. The two dominant grasses in
144 this lowland savanna (*Themeda triandra*, *Enteropogon macrostachyus*) are both perennial C_4 species; in
145 equatorial East Africa, C_3 grasses are restricted to high-mountain environments. Shrubs were defined as
146 woody plants with multiple stems, while trees had one erect woody stem. The lakeshore forest was
147 sampled at its northeastern end where the crater rim is lowest (ca. 60 m); savanna woodland on deep soils
148 outside the crater basin was sampled ca. 500 m to the northwest of the lake; and dry savanna woodland
149 on shallow rocky soils was sampled at the top of the western rim (ca. 180 m above lake level). A map
150 with the habitat locations relative to Lake Chala is given in Fig. 1.
151 In the three habitats we sampled the four (lakeshore), six (savanna) or eight (crater rim) locally most
152 abundant plant species, with the aim to achieve good representation of vegetation composition in each
153 habitat. Further, between two and four individual plant specimens (replicates) of each plant species were
154 sampled on each of the four collection dates. Four plant species (*Thylacium africanum*, *Vepris*
155 *uguenensis*, *Themeda triandra*, *Grewia tephrodermis*) were common in two of the three habitats (Table
156 1) and hence sampled in both, thereby allowing a separation of species and habitat effects.
157 Plant xylem tissue was sampled with two different techniques, depending on plant characteristics. For
158 trees with a diameter >10 cm, a core drill sample was extracted (diameter 4.30 mm, length 300 mm) and
159 the outer layer (epidermis, cortex, bark fibers, phloem) was removed to prevent contamination with
160 phloem sap. For smaller trees and shrubs, twig pieces were sampled and the outer layer was scraped off
161 using a knife. No xylem tissue was sampled from grasses. Xylem samples were stored in sealed glass
162 vials with rubber/PTFE liner until water extraction.
163 Plant leaves were sampled depending on plant growth form. For grasses, the whole above-ground
164 plant was sampled, which consisted entirely of green leaves. For trees and shrubs, fresh leaves were
165 randomly collected at different heights and at the four cardinal points (exposure towards north, east,
166 south, west) and merged into one composite sample representing the entire plant. Entire leaves were
167 collected to allow for intra-leaf variability (Helliker and Ehleringer, 2000; Sessions, 2006). All leaves

5

168   were sampled between 10AM and 3PM (UTC+3) to limit the effect of diurnal variation in transpiration
169   on the isotopic signature of leaf water (Cernusak et al., 2002; Li et al., 2006; Kahmen et al., 2008). For
170   leaf-water analysis, leaf samples were stored frozen until water extraction, while for leaf-wax *n*-alkane
171   analysis, leaf samples were kept in paper envelopes until dry for 7 days at 40 °C, subsequently ground
172   using a centrifugal mill (Retsch ZM 200) and stored in self-sealing LDPE bags until lipid extraction.

173   2.3. Leaf- and xylem-water extraction and isotopic analysis

174   Methods and results of leaf and xylem water analysis were presented by De Wispelaere et al. (2017).
175   In brief, leaf and xylem water was quantitatively extracted via cryogenic water vacuum distillation (West
176   et al., 2006). Following Araguás-Araguás et al. (1995), isotopic data were retained for interpretation only
177   if the extraction efficiency, determined by further drying of the sample at 105 °C for at least 48h,
178   exceeded 98%. The δ^2H of these water samples was determined using cavity ring-down spectrometry
179   (WS-CRDS, L2120-i, Picarro, USA), coupled with a vaporizing module (A0211 high-precision
180   vaporizer) and a micro-combustion module, which eliminates the interference of organic compounds
181   (Martín-Gómez et al., 2015). Each sample was measured 10 times, of which the first 5 injections were
182   eliminated in order to overcome memory effects. The measurement uncertainty (±1 σ) was 0.4‰.
183   Hydrogen-isotopic signatures are expressed using the delta (δ) notation, which is the relative
184   difference in isotopic ratio of the heavy isotope to the most abundant isotope (here, $^2H/^1H$) in the sample
185   (R_{sample}), relative to this same isotopic ratio of an international standard ($R_{standard}$) (Gat, 2010).

186
$$\boldsymbol{\delta} = \left(\frac{\boldsymbol{R_{sample} - R_{standard}}}{\boldsymbol{R_{standard}}}\right)$$

187   For stable hydrogen isotopes, the reference standard is Vienna Standard Mean Ocean Water
188   (VSMOW) which, by definition, has a δ^2H value of 0‰.

189   2.4. Lipid extraction and purification

190   Lipids were extracted from dried leaf samples using an accelerated solvent extractor (ASE 350,
191   Thermo Scientific, Bremen, Germany). Each extraction cell (type SST, 22 ml) was provided with top
192   and bottom pre-extracted cellulosic filters (27 mm), filled with 0.5-0.7 g ground leaf material and topped
193   up with diatomaceous earth (flux-calcined, Sigma-Aldrich). Extraction was performed with
194   dichloromethane:methanol (9:1, v:v) at 103 °C for at least three cycles of 6 min each and 60 % flush.
195   The solvent was evaporated to dryness under reduced pressure at 40 °C and re-dissolved in 3 ml *n*-
196   hexane. Total lipid extracts were transferred to a silica-gel column (Chromabond 6 ml SPE, filled with
197   500 mg of SiOH, Machery-Nagel) preconditioned with two times 4 ml *n*-hexane. The neutral fraction
198   (containing *n*-alkanes) was collected by elution with 4 ml *n*-hexane. Finally, the solvent was reduced in
199   volume and transferred to chromatography vials.

200   2.5. Hydrogen-isotopic analysis of leaf-wax *n*-alkanes

201   The hydrogen-isotopic signature of *n*-alkanes (in leaf waxes, δ^2H_{wax}) was measured by capillary gas
202   chromatography-thermal conversion-isotope ratio mass spectrometry (GC-TC-IRMS; Trace GC Ultra

interfaced via a GC/C III to a Delta^{PLUS} XP IRMS, Thermo Scientific, Bremen, Germany) equipped with a programmable temperature vaporizer (PTV) injector and a BPX 5 column (30 m x 0.25 mm x 0.5 µm, SGE, Milton Keynes, UK). Thermal conversion (pyrolysis) was done using a ceramic reactor kept at 1425°C and conditioned by injecting iso-octane in straight mode. H_3^+ was <6 ppm/nA and determined at least every second day assuring a H_3^+ drifter <0.03 ppm/nA/h. Samples were injected at least in duplicate and five consecutive samples were bracketed with four external laboratory reference mixtures of different concentration covering the concentration range of the samples. The laboratory reference mixtures were composed of odd n-alkanes from C_{25} to C_{35}, with δ^2H values ranging from -91.5‰ to 245.6‰ which was calibrated toward a certified reference mixture (A4) that is traceable to VSMOW, SLAP, NBS 19, and L-SVEC and was provided by Arndt Schimmelmann (Indiana University, USA). Combined uncertainty toward the VSMOW-SLAP scale for the laboratory standard was <2.5‰ (and <2.0‰ for five of the six alkanes). For samples, only chromatographic peaks in the linear range of the IRMS (1000 to 10,000 mV) were considered. At the start and end of each measurement, series of H_2 working-gas pulses were injected in the system, and used as temporary scale anchor between sample and reference-mixture measurements (Meier-Augenstein and Schimmelmann, 2019), resulting in an average combined uncertainty of 2.4‰ on the VSMOW-SLAP scale for δ^2H values of C_{29} and C_{31} alkanes in our plant samples. Prior to GC-TC-IRMS analysis, concentrations and peak purity of n-alkanes were determined using gas chromatography-mass spectroscopy (GC-MS; single quadrupole mass spectrometer, DSQ, Thermo Scientific, Germany coupled with a Trace GC). This pre-assessment was also used to adjust the volume of solvent to optimize n-alkane concentration, targeting 100 µg/mL before the GC-TC-IRMS isotope analysis. Peak purity was evaluated visually (absence of peak distortion and shoulders) and using the spectral deconvolution software AMDIS (AMDIS32 V2.1, National Institute of Standards and Technology Maryland, USA), setting the minimum purity index equal to 80 (Mallard, 2014).

In principle, the δ^2H_{wax} signature of each individual leaf-wax n-alkane compound can be suitable as paleohydrological proxy. However, calculating an abundance-weighted mean δ^2H_{wax} value to obtain one single integrated isotopic signature per measured sample has several advantages (Gao et al., 2014). First, including multiple homologues reduces the potential influence of outliers, increases the likelihood of obtaining representative isotopic data (homologues with high concentrations account for more) and gives a statistically more robust representation. Second, integration avoids data gaps when concentrations of certain individual compounds in a sample are too low for accurate isotopic measurement. In our study, δ^2H_{wax} of C_{29} and C_{31} (the two most abundant n-alkanes, see paragraph 3.1) showed strongly positive correlation (r_p = 0.88, p < 0.001, n = 126), justifying the use of an abundance-weighted mean of these two homologues. Thus, from here on, δ^2H_{wax} refers to the abundance-weighted mean δ^2H value of C_{29} and C_{31}. These two compounds are also the most commonly applied leaf-wax n-alkanes in non-marine paleohydrological research (Sachse et al., 2012 and references therein).

2.6. Hydrogen-isotopic enrichment

The isotopic enrichment $\varepsilon_{a/b}$ is the relative difference in isotopic ratio between source (R_b) and product (R_a) and represents the isotopic fractionation from (b) to (a). For hydrogen (^2H) it is computed as (Sachse et al., 2012):

242 $$\varepsilon_{a/b} = \frac{R_a - R_b}{R_b} = \left(\frac{\delta^2 H_a + 1}{\delta^2 H_b + 1} - 1\right)$$

243   In our study, we calculated the following hydrogen-isotopic enrichments: 1) $\varepsilon_{leaf/source}$ between the
244 hydrogen-isotopic signature of plant source water ($\delta^2 H_{source}$) and the hydrogen-isotopic signature of leaf
245 water ($\delta^2 H_{leaf}$); 2) ε_{bio} (i.e. $\varepsilon_{wax/leaf}$) between the hydrogen-isotopic signature of leaf water ($\delta^2 H_{leaf}$) and the
246 abundance-weighted average hydrogen-isotopic signature of C_{29} and C_{31} n-alkanes ($\delta^2 H_{wax}$); and 3) ε_{net}
247 (i.e. $\varepsilon_{wax/source}$) between the hydrogen-isotopic signature of plant source water ($\delta^2 H_{source}$) and the
248 abundance-weighted average hydrogen-isotopic signature of C_{29} and C_{31} n-alkanes ($\delta^2 H_{wax}$).
249   For plant source water three different water pools were used to compare the outcome of calculations:
250 1) volume-weighted mean annual precipitation with a hydrogen-isotopic signature of -6.5‰ (De
251 Wispelaere et al., 2017); 2) NE monsoon rainwater with an average hydrogen-isotopic signature of -
252 26.5‰ (De Wispelaere et al., 2017); and 3) hydrogen-isotopic signature of xylem water ($\delta^2 H_{xylem}$), which
253 varied from -87 to 25‰ (-17 ± 17‰, $n = 132$) throughout the year (this study).

254 **2.7. Leaf-wax *n*-alkane distribution patterns**

255   Terrestrial higher plants produce significant amounts of *n*-alkanes, with predominance of odd-
256 numbered carbon chains, of which typically one or two chain lengths dominate (Eglinton and Hamilton,
257 1967). A simple parameter to describe the *n*-alkane distribution pattern is the average chain length (ACL).
258 It represents the abundance-weighted average chain length of the different carbon compounds (Freeman
259 and Pancost, 2014). The odd-over-even ratio of carbon chain lengths is expressed as the carbon
260 preference index (CPI). The CPI of *n*-alkanes is often used to discriminate between fresh biogenic and
261 petrogenic contributions, as the latter lack a strong odd-number dominance (Freeman and Pancost, 2014),
262 while terrestrial higher plants typically produce *n*-alkanes with CPI values considerable higher than 1
263 (Eglinton and Hamilton, 1967; Rieley et al., 1991). ACL and CPI were here calculated as follows:

264 $$ACL_{27-33} = \sum (n \cdot C_n) / \sum (C_n)$$

265 $$CPI_{27-33} = \left[2 \cdot \sum_{odd} (C_{27-33})\right] / \left[\sum_{even} (C_{26-32}) + \sum_{even} (C_{28-34})\right]$$

266   with C_n being the concentration of each compound with *n* carbon atoms (Bray and Evans, 1961;
267 Freeman and Pancost, 2014).

268 **2.8. Statistical analyses**

269   In general, presented data refer to the observed mean value along with the standard deviation (SD)
270 and number of observations (n). Analysis of variance was performed for comparisons among plant
271 growth form, habitat and season. Tukey's post-hoc comparisons were used to examine the significance
272 of differences between selected groups of samples. A cut-off value of $p < 0.05$ was used to indicate
273 significant differences. These statistical analyses were performed with IBM SPSS Statistics software
274 (Version 24, IBM Corporation, 2016).

In further statistical analysis, we fitted mixed-effect models with respectively ACL, CPI, $C_{31}/(C_{29}+C_{31})$ ratio, δ^2H_{leaf}, δ^2H_{wax} and ε_{bio} as response variables. In this setup we used growth form, habitat and season as fixed effects, with a random error structure, and introduced the sampled plant species as a random effect, as the species themselves represent a randomly drawn sample from the pool of common species present at each location. Models were then fitted using maximum-likelihood methods in the 'lme4' package in R (Bates et al., 2015). Finally, the marginal and conditional R^2 were calculated for all models, which indicate the proportion of the variance that is explained, respectively, by the fixed structure and the fixed and random structures together (Nakagawa and Schielzeth, 2013). Differences between marginal (fixed effects) and conditional (overall model) R^2 gives the proportion of variance explained by random (species) effects. All analysis were done using R software (R Core Team, 2018).

3. RESULTS

3.1. Leaf-wax *n*-alkane distribution patterns among plant growth forms, habitats and seasons

Carbon chain lengths of *n*-alkane compounds in plant leaves ranged from C_{21} to C_{35}, with the dominant *n*-alkanes being the odd homologues C_{27} to C_{33} (combined relative abundance $88.0 \pm 10.4\%$, $n = 209$, Supplementary Fig. 1), resulting in ACL values ranging between 28.3 and 31.9, with an overall average of 30.2 ± 0.9 ($n = 209$). Variation in ACL values among replicates of the same species (separate per habitat and season, and expressed as standard deviation normalized to overall ACL range) was $6.5 \pm 6.0\%$ (Supplementary Fig. 2). ACL values were significantly influenced by growth form ($p < 0.001$), with ACL values of shrubs (30.0 ± 1.0, $n = 107$) being slightly lower than those of grasses (30.8 ± 0.4, $n = 20$, $p < 0.001$) and trees (30.4 ± 0.6, $n = 64$, $p < 0.01$). Habitat and season had no significant effect on ACL values overall ($p = 1.00$ and $p = 0.31$, respectively). The linear mixed-effect model for ACL explained 79% of the overall variability, with 18% allocated to fixed effects (growth form, habitat, season) and 61% to random (i.e. species) effects (Table 2). Parameter estimates of fixed effects were higher for growth form compared to habitat and season (Table 2) and confirm that only growth form influenced ACL values.

All 14 plant species in our study showed a predominance of odd over even carbon numbers (CPI values ranging between 1.6 and 50.1, $n = 188$), with an overall mean CPI value of 12.8 ± 8.7. Variation in CPI among replicates of the same species was $7.3 \pm 7.1\%$ (Supplementary Fig. 2). One shrub species (*Thylachium africanum*) had an exceptionally low CPI value of 2.6 ± 0.8 ($n = 18$, including specimens from crater rim and lakeshore). CPI values were significantly different between all growth forms ($p < 0.001$) with highest values for grasses (23.9 ± 9.5, $n = 20$) followed by trees (15.0 ± 6.4, $n = 60$) and shrubs (9.2 ± 6.4, $n = 102$; Fig. 2). Habitat had no significant effect on CPI values overall ($p = 0.95$). CPI values were significantly different ($p < 0.01$) between the two rainy seasons, with higher values for the NE monsoon rains (17.1 ± 11.9, $n = 33$) compared to the SE monsoon rains (10.2 ± 7.0, $n = 48$), especially in grasses (Fig. 2). Dry-season CPI values were intermediate between those of the two rainy seasons, and not significantly different from each other ($p = 1.00$), for all growth forms. The linear mixed-effect model for CPI explained 61% of the overall variability, with 29% allocated to fixed effects (growth form, habitat, season) and 33% to random effects (Table 2). Parameter estimates of fixed effects showed higher values for growth form compared to habitat and season (Table 2), confirming the stronger influence of growth form on CPI values.

315   The ratio of $C_{31}/(C_{29}+C_{31})$ averaged over all plant types, habitats and seasons equaled 0.57 ± 0.24
316   (ranging between 0.01 and 1.00, $n = 209$). Variation in $C_{31}/(C_{29}+C_{31})$ ratio among replicates of the same
317   species was $5.9 \pm 7.1\%$ (Supplementary Fig. 2). Growth form significantly influenced the $C_{31}/(C_{29}+C_{31})$
318   ratio ($p < 0.001$) with shrubs showing lowest values (0.50 ± 0.25, $n = 120$), followed by trees ($0.62 \pm$
319   0.21, $n = 66$) and highest values for grasses (0.79 ± 0.07, $n = 23$; Fig. 3). Note that the significance of
320   this effect is not affected by the difference in sample size between the three growth forms ($p < 0.001$ also
321   when n in shrubs and trees is reduced to 23 via random selection). Habitat and season had no significant
322   effect on the $C_{31}/(C_{29}+C_{31})$ ratio ($p = 0.90$ and $p = 0.58$, respectively). The linear mixed-effect model for
323   the $C_{31}/(C_{29}+C_{31})$ ratio explained 66% of the overall variability, with 19% allocated to fixed effects
324   (growth form, habitat, season) and 47% to random effects (Table 2). Parameter estimates of fixed effects
325   showed higher values for growth form compared to habitat and season (Table 2), confirming the stronger
326   influence of growth form on the $C_{31}/(C_{29}+C_{31})$ ratio.

327 **3.2. Leaf-wax *n*-alkane δ²H variation among plant growth forms, habitats and seasons**

328   Averaged over all plant types, habitats and seasons δ²H$_{wax}$ equaled -126.4 $\pm$ 26.5‰ (ranging between
329   -202.4 and -70.9‰, $n = 165$; Fig. 4). Variation in δ²H$_{wax}$ among replicates of the same species was 4.7 $\pm$
330   4.8% (Supplementary Fig. 2).
331   Growth form significantly influenced the δ²H$_{wax}$ signature ($p < 0.001$), with grasses exhibiting on
332   average the most depleted values (-163.5 $\pm$ 15.2‰, $n = 23$) followed by shrubs (-123.8 $\pm$ 22.7‰, $n = 96$)
333   and trees (-113.1 $\pm$ 21.5‰, $n = 46$). At the level of individual species, *Boswellia neglecta* (the only tree
334   commonly occurring on the crater rim; Table 1) had leaf waxes relatively strongly ^{2}H-depleted for a tree,
335   whereas those of the shrub *Maerua* sp. are even less depleted than most trees (Fig. 4). δ²H$_{wax}$ values also
336   depended significantly on habitat, with on average less depleted values at the lakeshore (-106.1 $\pm$ 16.5‰,
337    $n = 34$) than on the crater rim (-129.2 $\pm$ 24.1‰, $n = 87$, $p < 0.001$) and in the savanna (-136.4 $\pm$ 29.5‰,
338    $n = 44$, $p < 0.001$). At least part of this effect is due to the fact that grasses are uncommon in the lakeshore
339   forest, and hence were not sampled (Supplementary Fig. 3a). In line with this observation, the compound
340   δ²H$_{wax}$ signature of crater rim and savanna vegetation was not significantly different ($p = 0.26$). On the
341   other hand, δ²H$_{wax}$ values for *Thylachium africanum* shrubs sampled at the lakeshore were also less
342   depleted than those sampled on the crater rim (respectively -113.1 $\pm$ 9.3‰, $n = 7$; and -122.2 $\pm$ 12.9‰,
343    $n =11$), although the difference between them is not significant ($p = 0.13$). The two shrub species sampled
344   both in savanna and on the crater rim (*Grewia tephrodermis* and *Vepris uguenensis*) have more similar
345   δ²H$_{wax}$ values in both habitats ($p = 0.21$ and $p = 0.53$, respectively), i.e. consistent with the compound
346   δ²H$_{wax}$ values of these two habitats as a whole also being similar. Further, leaf waxes of the grass
347   *Themeda triandra* were significantly more ^{2}H-depleted in the savanna than on the crater rim ($p < 0.001$;
348   Supplementary Fig. 3a), and are by themselves mainly responsible for the difference in compound δ²H$_{wax}$
349   values between these two habitats as represented in this study (Fig. 4).
350   The influence of season on δ²H$_{wax}$ differs among growth forms and habitats. On the crater rim, δ²H$_{wax}$
351   signatures are relatively constant throughout the four seasons in all three growth forms (Supplementary
352   Fig. 3a), with the greater isotopic variability among shrub samples reflecting the greater number of
353   species sampled (six, compared to one each in grasses and trees). In the savanna and lakeshore forest,
354   δ²H$_{wax}$ signatures vary more strongly between seasons but with no consistent pattern across the three
355   growth forms or across these two habitats (Supplementary Fig. 3a). As a result, season had no significant

effect on δ^2H_{wax} values overall ($p = 0.11$) nor in each of the three habitats separately ($p = 0.14 - 0.79$; Supplementary Fig. 3b).

The linear mixed-effect model for δ^2H_{wax} explained 80% of the overall variability, with 40% allocated to fixed effects (growth form, habitat, season) and 39% to random effects (Table 2). Parameter estimates of fixed effects again showed higher values for growth form compared to habitat and season (Table 2), confirming the stronger influence of growth form on δ^2H_{wax} values than habitat or season.

3.3. Xylem-water δ^2H variation among plant growth forms, habitats and seasons

The hydrogen-isotopic signatures of xylem water (δ^2H_{xylem}) in seven shrub and five tree species from our study region (no data for grasses, see Methods) ranged from -86.9 to +25.1‰ (Fig. 5), with an overall mean δ^2H_{xylem} value of -17.1 ± 17.2‰ ($n = 132$), i.e. overall markedly less depleted in ^2H than the leaf waxes of those same plants ($p < 0.001$; compare with Fig. 4). Variation in δ^2H_{xylem} values among replicates of the same species was 4.9 ± 6.6% (Supplementary Fig. 2).

As in the leaf waxes, growth form significantly affected the δ^2H_{xylem} signature ($p < 0.001$) with shrubs (-23.3 ± 15.2‰, $n = 81$) again showing lower values, on average, than trees (-7.2 ± 15.6‰, $n = 51$). Also habitat significantly affected δ^2H_{xylem} values ($p < 0.001$), again with lakeshore plants (-0.8 ± 10.2‰, $n = 42$) showing higher values, on average, than plants on the crater rim (-24.9 ± 15.2‰, $n = 60$) and in the savanna (-24.1 ± 12.4‰, $n = 30$), and the latter not being significantly different from each other ($p = 0.97$). Separation of data on growth form and habitat (Supplementary Fig. 4a) shows that the above patterns are mostly due to the isotopically enriched xylem water of lakeshore trees (1.7 ± 9.1‰, $n = 34$), compared to all other shrubs and trees (-23.6 ± 14.3‰, $n = 98$). Note that the relatively enriched compound δ^2H_{xylem} signature of lakeshore vegetation cannot be attributed to the lack of grasses in this habitat. Also here, the δ^2H_{xylem} values of *Thylachium africanum* shrubs sampled at the lakeshore were less depleted than those sampled on the crater rim (respectively -11.3 ± 7.9‰ and -20.5 ± 7.0‰) and this time the difference between them is significant ($p < 0.05$). The two shrub species sampled both in savanna and on the crater rim (*Grewia tephrodermis* and *Vepris uguenensis*) have more similar δ^2H_{xylem} values in the two habitats ($p = 0.72$ and $p = 0.37$, respectively), i.e. consistent with also the compound δ^2H_{xylem} values of these two habitats as a whole being similar.

As in the leaf waxes, the influence of season on the ^2H-isotopic signature of xylem water is statistically not significant ($p = 0.06$), however the near-significance of this overall result stimulates a detailed look at underlying structure in the δ^2H_{xylem} data (Supplementary Figs. 4a-b). This fails to show a common trend, except that the isotopically most depleted xylem water was recorded during either the NE monsoon season (crater rim, savanna) or the long dry season (lakeshore); and that in the savanna habitat, xylem water sampled during the short dry season was less depleted than that sampled during the preceding NE monsoon season ($p < 0.05$).

3.4. Leaf-water δ^2H variation among plant growth forms, habitats and seasons

The hydrogen-isotopic signatures of leaf water (δ^2H_{leaf}) in 14 plant species from our study region ranged from -82.7 to +35.5‰ (Fig. 6), with an overall mean value of +3.6 ± 20.3‰ ($n = 156$), i.e. significantly enriched relative to the xylem water of those same plants ($p < 0.001$). Variation in δ^2H_{leaf}

394   among replicates of the same species was 6.2 ± 5.6%, i.e. somewhat larger than the equivalent values for
395   δ^2H_{wax} and δ^2H_{xylem} (Supplementary Fig. 2) but not significantly so ($p = 0.39$ and 0.56, respectively).
396   In contrast with the xylem water and leaf waxes, growth form did not have a statistically significant
397   influence on δ^2H_{leaf} values overall ($p = 0.16$). This lack of effect may be attributed partly to leaf water of
398   the shrub *Maerua* sp. on the crater rim being markedly depleted relative to its xylem water rather than
399   enriched (compare with Fig. 5), and δ^2H_{leaf} of the grass *Themeda triandra* on the crater rim overlapping
400   more strongly with those of crater rim shrubs, then is the case in their respective δ^2H_{wax} signatures
401   (compare with Fig. 4). Nevertheless, removing these two plant species from the dataset does not enhance
402   the effect of growth form on δ^2H_{leaf} ($p = 0.88$). The compound δ^2H_{leaf} values of crater-rim (+0.2 ± 23.7‰,
403   $n = 67$) and savanna vegetation (+10.1 ± 12.1‰, $n = 49$) are statistically different ($p < 0.05$), but this is
404   entirely on account of the exceptionally depleted δ^2H_{leaf} values in *Maerua* sp. (-56.7 ± 13.6‰, $n = 6$; Fig.
405   6); excluding this species, the difference is not significant ($p = 0.35$). As regards the three plant species
406   sampled in both habitats (*Grewia tephrodermis*, *Themeda triandra*, *Vepris uguenensis*), no significant
407   difference was observed between habitats ($p = 0.29$, 0.10 and 0.12, respectively). Further, no overall
408   difference was observed between lakeshore (1.2 ± 20.7‰, $n = 40$) and crater rim ($p = 0.97$) or savanna
409   habitats ($p = 0.09$), nor between *Thylachium africanum* sampled on the crater rim and at the lakeshore (p
410   = 0.57).
411   Average δ^2H_{leaf} values separated out per growth form and habitat (Supplementary Fig. 5a) appear to
412   suggest marked seasonality in all situations except in savanna shrubs, but with no consistent seasonal
413   trend among the habitats (Supplementary Fig. 5b). As a result, there is no significant effect of season on
414   δ^2H_{leaf} values overall ($p = 0.32$).
415   The linear mixed-effect model for δ^2H_{leaf} explained 69% of the overall variability with only 8%
416   allocated to fixed effects (growth form, habitat, season) and 61% to random effects (Table 2). Parameter
417   estimates of fixed effects were in a similar range (Table 2) and confirm that none of the tested effects
418   (growth form, habitat, season) had a pronounced influence on δ^2H_{leaf}.

419   **3.5. Biosynthetic enrichment among plant growth forms, habitats and seasons**

420   The biosynthetic enrichment factor (ε_{bio}) ranged from -193.7 to -19.6‰ across our dataset (Fig. 7),
421   with an overall mean value of -131.0 ± 32.9‰ ($n = 121$). Variation in ε_{bio} among replicates of the same
422   species was 5.1 ± 4.1% (Supplementary Fig. 2).
423   Variation in ε_{bio} among species was significantly influenced by growth form with grasses (-162.8 ±
424   17.0‰, $n = 17$) showing more negative values than shrubs (-128.4 ± 35.2‰, $n = 69$, $p < 0.001$) and trees
425   (-120.5 ± 23.6‰, $n = 35$, $p < 0.001$), in a pattern mainly reflecting the variation among species observed
426   in δ^2H_{wax} (compare with Fig. 4). In the case of the shrubs, the difference with grasses remains highly
427   significant ($p < 0.001$) also after excluding the outlying values obtained for *Maerua* sp. (-27.9 ± 8.3‰,
428   $n = 4$). However, in contrast to the compound isotopic signatures of leaf waxes (and xylem water) the
429   overall difference in ε_{bio} between shrubs and trees was not significant ($p = 0.42$). At the level of individual
430   species, outlying ε_{bio} values (e.g., *Boswellia neglecta*, *Maerua* sp.) reflect similar positions of these
431   species in either δ^2H_{wax} or δ^2H_{leaf} signatures. Also mirroring the δ^2H_{wax} trends, ε_{bio} was significantly
432   influenced by habitat with plants at the lakeshore showing less negative values on average (-108.0 ±
433   16.5‰, $n = 24$) than those on the crater rim (-130.5 ± 35.1‰, $n = 61$, $p < 0.01$) or in the savanna (-147.0
434   ± 28.0‰, $n = 36$, $p < 0.001$). Also the compound ε_{bio} values of crater rim and savanna were significantly

435   different ($p < 0.05$), but as in δ^2H_{leaf} (Fig. 6) this is entirely on account of *Maerua* sp. (-27.9 ± 8.3‰, $n =$
436   4; Fig. 7). None of the four species sampled in two different habitats (*Grewia tephrodermis*, *Themeda*
437   *triandra*, *Thylachium africanum*, *Vepris uguenensis*) showed a significant difference in ϵ_{bio} between
438   those habitats (all $p > 0.05$). Again, also season did not significantly affect ϵ_{bio} ($p = 0.22$), due to lack of
439   uniform seasonal trends among the three habitats (Supplementary Fig. 6a-b).

440   The linear mixed-effect model for ϵ_{bio} explained 83% of the overall variability, with 19% allocated to
441   fixed effects (growth form, habitat, season) and 63% to random effects (Table 2). Parameter estimates of
442   fixed effects showed higher values for growth form compared to habitat and season (Table 2), suggesting
443   a stronger influence of growth form on ϵ_{bio} than habitat or season, as is the case in δ^2H_{wax}.

4. DISCUSSION

4.1. Distribution patterns of leaf-wax *n*-alkanes

446   The distribution patterns of individual *n*-alkane compounds that we observed in fresh leaves of plant
447   species around Lake Chala are typical for cuticular waxes of terrestrial vascular plants (Eglinton and
448   Hamilton, 1967) and have been observed previously in plant species of tropical African savannas
449   (Rommerskirchen et al., 2006; Vogts et al., 2009; Bush and McInerney, 2013). Parameters describing
450   these *n*-alkane distributions (ACL, CPI and the $C_{31}/(C_{29}+C_{31})$ ratio; Bush and McInerney, 2013; Freeman
451   and Pancost, 2014) were all significantly affected by growth form, with grasses exhibiting highest values
452   for all parameters mostly because in grasses the C_{31} *n*-alkane is ca. four times more abundant than the
453   C_{29} *n*-alkane, whereas in trees and shrubs their abundances are similar (Supplementary Fig. 1). ACL and
454   CPI have previously been shown to vary with growth form and therefore reflect variation in plant
455   community composition, although not in a simple or systematic way (Diefendorf et al., 2011). Also the
456   abundance ratios of individual *n*-alkane compounds differ between specific groups of vascular plants.
457   Specifically, the C_{29} and C_{31} *n*-alkane tend to co-dominate in woody plants while C_{31} is more dominant
458   in grasses (Chikaraishi and Naraoka, 2007; Vogts et al., 2009). Thus, the $C_{31}/(C_{29}+C_{31})$ ratio of *n*-alkanes
459   extracted from soil and lake records has been used as proxy to reconstruct long-term shifts in the relative
460   abundance of grasses versus woody plants in the tropical Andes of Ecuador (Jansen et al., 2008) and on
461   the north slope of Mt. Kilimanjaro (Zech et al., 2011). Also in our study area on the lower southeast slope
462   of Mt. Kilimanjaro, when averaged across all habitats and seasons, grasses exhibit a significantly higher
463   $C_{31}/(C_{29}+C_{31})$ ratio than woody plants (Fig. 3). Based on our data, this ratio even appears promising to
464   separate shrubs from trees ($p < 0.001$); however the numerical difference is small and species-specific
465   values span wide ranges (respectively 0.50 ± 0.25 and 0.62 ± 0.21), so whether this result is robust against
466   a different selection of analysed shrub and tree species remains to be confirmed. Moreover, as
467   $C_{31}/(C_{29}+C_{31})$ values in paleo-records will always reflect a mixture of grasses, shrubs and trees,
468   inferences can do no better than referring to the end members 'grass' and 'non-grass'. Nevertheless, our
469   data support the case presented by Zech et al. (2011) that the *n*-alkane $C_{31}/(C_{29}+C_{31})$ ratio combined with
470   ACL and CPI can be a useful tool in East African paleoecological studies to trace past changes in the
471   relative land cover of grasses versus woody plants. In this context, also Bush and McInerney (2013)
472   found that grasses in Sub-Saharan Africa (i.e., on a continental scale) are distinguishable from woody
473   plants based on the relative abundance of C_{29} and C_{31}, while this is not the case on the global scale.

Habitat and season did not significantly affect *n*-alkane distribution patterns, except for those reflected in the CPIs, which were significantly different during the NE and SE monsoon seasons, and most strikingly so in grasses (Fig. 2). To our knowledge, no data in the current literature exist to help explain this result or provide context for it. Previous research on the influence of climate or seasonality on *n*-alkane distribution patterns seems to have focused on variations in temperature, which in our study region are likely too modest to control *n*-alkane distribution at the seasonal time scale. Working in North America, Bush and McInerney (2015) documented influence of temperature on ACL values along a latitudinal transect under uniform precipitation. However, alternative data compilation by Diefendorf and Freimuth (2017) showed that a temperature effect on ACL values was only apparent for C_4 grasses, not for C_3 grasses or woody plants.

4.2. What drives δ^2H_{wax} variability in plants?

The overall range in δ^2H_{wax} values among plant species sampled in our study region can be attributed partly to the use of different water sources, and partly to processes preceding and accompanying *n*-alkane biosynthesis (see Introduction). The relative influence of each process, however, is often quite uncertain (Sessions, 2016). In the following, we discuss the effects, and estimate the relative importance, of plant growth form, habitat and season on the isotopic signature of plant source water (i.e. xylem water), leaf water and biosynthetic fractionation in our study area, as well as their relation to the isotopic signature of leaf-wax *n*-alkanes.

4.2.1. The isotopic signature of plant source water (δ^2H_{xylem})

In a previous study, we analyzed xylem water of exactly the same plants across the same set of habitats and seasons at Lake Chala (De Wispelaere et al., 2017). As water uptake through the roots is generally considered to occur without isotopic fractionation (White et al., 1985; Zhao et al., 2016), the isotopic signature of xylem water (δ^2H_{xylem}) was assumed to reflect the isotopic signature of the plant's source water. The range of average δ^2H_{xylem} values between the crater rim, lakeshore and savanna habitats, integrated across all locally sampled plants and seasons (24.1‰, Fig. 5) is comparable to that in δ^2H_{wax} values between these same habitats (19.0‰, restricted to shrubs and trees for comparability; Fig. 4) and both are significantly influenced by habitat ($p < 0.001$). The isotopically most enriched δ^2H_{wax} values occur in plants at the lakeshore, which could be expected since they rely on lake water which is isotopically enriched due to continuously strong evaporation from the lake surface (Payne, 1970; Barker et al., 2011). In addition the hydrological budget of Lake Chala depends on large inflows of groundwater originating from percolation of rainfall higher up on Mt. Kilimanjaro (Verschuren et al., 2009). The hydrogen-isotopic signature of this groundwater integrates multiple sources of precipitation, whereas plants on the crater rim and in savannah outside the crater largely rely on soil water derived from isotopically more strongly depleted precipitation of the NE monsoon (De Wispelaere et al., 2017). Although interspecies variability in δ^2H_{wax} is large, we find limited species overlap between the lakeshore and other habitats (Fig. 4). Moreover the significant difference between δ^2H_{xylem} values of *Thylachium africanum* growing in lakeshore and crater rim habitats (respectively -11.3 ± 7.9‰ and -20.5 ± 7.0‰; $p < 0.05$) largely survives in its δ^2H_{wax} signature (respectively -113.1 ± 9.3‰ and -122.2 ± 12.9‰, $p = 0.13$; Fig. 4). The fact that the latter difference fails to reach statistical significance, if not due to the

513   modest sample sizes (n = 7-11) pertaining to this comparison, likely points to the controls of leaf-water
514   transpiration ($\varepsilon_{leaf/xylem}$) and biosynthetic fractionation (ε_{bio}) on δ^2H_{wax}.

515   De Wispelaere et al. (2017) also found that xylem water of plants around Lake Chala does not trace
516   the large seasonal variation in the isotopic signature of precipitation, but that the short NE monsoon rains
517   are the primary source of water for those plants throughout the year, implying that these rains fully
518   recharge the soil water pools which have become depleted during the long dry season. The fact that plants
519   access this single water source throughout the year may partly explain why δ^2H_{xylem} and δ^2H_{wax}, when
520   pooled across growth forms and habitats, do not appear to be significantly affected by season ($p > 0.05$).
521   However, our analysis shows that this apparent lack of influence reflects lack of a consistent seasonal
522   pattern in δ^2H_{xylem} and δ^2H_{wax} among growth forms and habitats, rather than that their values are uniform
523   throughout the year (Supplementary Figs. 3-4). Nevertheless arguing in favor of the single water-source
524   hypothesis, we note that the range in δ^2H_{xylem} values recorded across all four seasons and all 11 plant
525   species sampled in the savanna and on the crater rim (-41.3 to +9.4‰; n = 83; this excludes seven outlier
526   data [see Fig. 5] as well as all lakeshore plants because they partly use evaporated lake water) is
527   significantly narrower than variation in the hydrogen-isotopic signature of local rainfall recorded during
528   the study period (-47.9 to +36.6‰; De Wispelaere et al., 2017). These δ^2H_{xylem} values are also more
529   similar to the average NE monsoon value (-26.5 $\pm$ 21.5‰; n = 2) than to the average SE monsoon value
530   (+16.0 $\pm$ 2.5‰; n = 3). In any event, it is clear that the isotopic signature of plant source water (here
531   represented by δ^2H_{xylem}) does not fully explain the broad range in δ^2H_{wax} observed in our study area.

532   **4.2.2. The isotopic signature of leaf water (δ^2H_{leaf})**

533   The isotopic signature of leaf water (δ^2H_{leaf}) is not only determined by the plant's source water, but
534   also other variables such as local air temperature and relative humidity through their influence on leaf
535   transpiration (Cernusak et al., 2016), which itself is also expected to depend on plant-specific features
536   such as growth form (Gao et al., 2014). However, our results show that δ^2H_{leaf} values in the Lake Chala
537   area are not significantly influenced by growth form, but (as are both δ^2H_{xylem} and δ^2H_{wax}) significantly
538   influenced by habitat. However, for δ^2H_{leaf} this held true *only* for the crater rim versus savanna, whereas
539   for δ^2H_{wax} it held true *except* for crater rim versus savanna. The fact that δ^2H_{leaf} values from the lakeshore
540   are not systematically different from those in the other habitats, despite them drawing their source water
541   mainly from isotopically more enriched lake water (De Wispelaere et al., 2017), suggest that other factors
542   (e.g., reduced transpiration in the relatively moist lakeshore habitat) overshadow the ^{2}H-isotopic
543   signature of the water source. Further, integrated over habitats and growth forms δ^2H_{leaf} was not
544   significantly influenced by season, which is in line with the data for δ^2H_{xylem} (source water) and δ^2H_{wax},
545   and can again be related to the fact that plants in our study area exploit specific water sources throughout
546   the year (lake water at the lakeshore, and NE monsoon rainwater on the crater rim and in the savanna).
547   Overall, there was no correlation between δ^2H_{leaf} and δ^2H_{wax} (r_p = 0.04, p = 0.69, n = 121, non-pooled
548   individual data pairs), consistent with other studies finding no significant effect of leaf transpiration on
549   δ^2H_{wax} (Hou et al., 2008; McInerney et al., 2011; Feakins et al., 2016).
550   The mixed-effect model result for δ^2H_{wax} explains more variability overall than is the case for δ^2H_{leaf}
551   (80% versus 69%) and with the fixed effects having considerably greater explanatory power (40% versus
552   8%; Table 2). Also the parameter estimates for growth form are considerably higher in the model output
553   for δ^2H_{wax} than in those for δ^2H_{leaf} (Table 2). These results, together with those above indicating that the

554 isotopic signature of source water (i.e., δ^2H_{xylem}) is also found in δ^2H_{wax} but appears to pass over δ^2H_{leaf},
555 may be explained by the fact that δ^2H_{wax} data integrate over longer periods of time compared to δ^2H_{leaf}
556 data, whereas the latter reflect large temporal (diurnal and longer-term) weather-related variability in leaf
557 transpiration. This conclusion is, to some extent, supported by our data on normalized variability (ratio
558 of SD over the total range of recorded values) in δ^2H_{leaf} being larger than in δ^2H_{wax} or δ^2H_{xylem}
559 (Supplementary Fig. 2). In this context, it must again be noted that obtaining a uniform dataset of δ^2H_{leaf}
560 from a large number of plants in the field is difficult, given the substantial diurnal variation in δ^2H_{leaf}
561 observed in single plants under controlled conditions (Cernusak et al., 2002; Li et al., 2006; Kahmen et
562 al., 2008). Although we only sampled leaves between 10AM and 3PM to limit this source of variability,
563 we acknowledge that this procedure may not have reduced it to negligible levels. Moreover the alternative
564 approach of using simulated mean-growing-season values of mid-day leaf-water δ^2H (cf. Kahmen et al.,
565 2013) is unfeasible due to the difficulty of obtaining the required imput data (ambient climatic variables,
566 δ^2H of atmospheric water vapor) at our study sites.

567 **4.2.3. Biosynthetic fractionation (ε_{bio})**

568 Leaf water (and in some plants, xylem water) is the ultimate source of hydrogen for the synthesis of
569 organic compounds during photosynthesis in higher plants (Sachse et al., 2012). Organic compounds are
570 usually strongly depleted in hydrogen compared to leaf water (up to -400‰, with variability up to 200‰
571 for the same homologous compounds; Sachse et al., 2012), because hydrogen-transfer reactions during
572 biosynthesis lead to strong hydrogen-isotopic fractionation (e.g., Sessions et al., 1999). Apart from
573 differences in metabolic pathways and hydrogen-transfer reactions (including exchange with
574 nicotinamide adenine dinucleotide phosphate, NADPH), also extrinsic environmental factors such as
575 temperature, drought stress, light intensity and growth rate can influence hydrogen-isotopic fractionation
576 during lipid biosynthesis (Shepherd and Griffiths, 2006). However, this influence of external factors on
577 lipid biosynthesis is currently not well understood and requires more systematic study (Sachse et al.,
578 2012; Eley et al., 2014; Newberry et al., 2015).
579 Our results showed that biosynthetic fractionation (ε_{bio}) was distinct among growth forms, with
580 grasses showing on average larger ε_{bio} values (-162 ± 17‰, $n = 17$) than shrubs and trees (-125 ± 32‰,
581 $n = 104$, $p < 0.001$), although variability among species within the latter two groups is very large (Fig.
582 7). If these compound isotopic signatures are indeed distinct, this may be due to differences in metabolic
583 pathway between the monocotyledonous grasses (both species analyzed here are C_4) and the
584 dicotyledonous trees and shrubs which use either C_3 or CAM (Crassulacean Acid Metabolism)
585 photosynthesis. Apart from their metabolic pathways, mono- and dicotyledonous plants also differ in leaf
586 architecture as well as the location and timing of biosynthesis. Also other studies targeting a broad range
587 of plant species (Liu et al., 2016; Sessions, 2016) observed substantial variability in ε_{bio} among growth
588 forms (grasses, shrubs, trees), mono- versus dicotyledonous plants, and C_3 versus C_4 plants.
589 Habitat also significantly affected ε_{bio}, with lakeshore showing the smallest compound value followed
590 by crater rim and savanna. Here it must be noted that since no grasses commonly occur at the lakeshore,
591 and were hence not sampled, the compound habitat effect may largely reflect the difference in proportion
592 of plant growth forms among the habitats. In any event, none of the four plant species sampled in two
593 habitats (cf. above) showed a significant difference in ε_{bio} between habitats, not even *Thylachium*
594 *africanum*. These results suggest that, firstly, the habitat effect on ε_{bio} mainly reflects the habitat effect

595   on $\delta^2 H_{wax}$; and secondly, that the compound ε_{bio} value of a habitat is to a large extent determined by its

596   plant species (and hence growth form) composition, possibly more so than habitat-specific factors such

597   as a difference in source water (cf. discussions of $\delta^2 H_{xylem}$ and $\delta^2 H_{leaf}$ above).

598   In line with the results discussed in previous sections and paragraphs, our linear mixed-effect model

599   explains 83% of the overall variability in ε_{bio}, i.e. comparable to the value for $\delta^2 H_{wax}$ (80%); however

600   here the largest part of this explained variability can be attributed to random species effects, as in $\delta^2 H_{leaf}$

601   but not $\delta^2 H_{wax}$. Conversely, model parameter estimates show that in the (modest fraction of) variability

602   explained by fixed effects, growth form exerted the strongest influence, as in $\delta^2 H_{wax}$ (Table 2).

4.3. Implications for paleohydrological studies using leaf-wax *n*-alkanes

604   Paleohydrological studies infer past temporal variation in regional hydroclimate from changes in the

605   (integrated) hydrogen-isotopic signature of leaf waxes extracted from lake sediments, in tropical East

606   Africa (e.g., Tierney et al., 2011; Berke et al., 2012; Costa et al., 2014) and elsewhere (e.g., Schefuß et

607   al., 2005; Garcin et al., 2018). In support of such paleohydrological inferences, our results show that

608   patterns in the isotopic signature of plants' leaf waxes across growth forms and habitats to a large extent

609   reflect the isotopic signature of their source water (as represented by $\delta^2 H_{xylem}$). Our results further suggest

610   that the regional 'net' (or 'apparent') hydrogen-isotopic enrichment between the plants' source water and

611   leaf-wax *n*-alkanes (ε_{net} or $\varepsilon_{wax/xylem}$), if validly assumed to have been constant through time, can under

612   certain conditions (cf. below) be employed to infer the ^2H signature of past precipitation.

613   Averaged over all plant growth forms (excluding grasses, since for grasses no xylem water data is

614   available), habitats and seasons, we find an overall ε_{net} value of -102 ± 30‰ for the Lake Chala area

615   when using xylem water as proxy for the plants' source water, i.e. significantly smaller ($p < 0.001$) than

616   when the plants' source water is weighted-average annual precipitation (-115 ± 23‰; excluding grasses

617   for comparability; Fig. 8). Notably, this difference dissolves ($p = 0.21$) when the ε_{net} value is calculated

618   on the basis of modern-day local NE monsoon rainwater (-96 ± 23‰) in all four seasons. This result

619   further corroborates the finding of De Wispelaere et al. (2017) that plants in the Chala region generally

620   use NE monsoon rainwater throughout the year. Finally, our compound ε_{net} value for the Lake Chala area

621   (calculated from either xylem water or NE monsoon rainwater data) is comparable with the ε_{net} value of

622   -94 ± 21‰ reported by Feakins and Sessions (2010) from a region in southern California with similar

623   semi-arid subtropical climate; however the discussion above should drive home the point that

624   interregional comparisons of this nature are necessarily highly tentative.

5. SUMMARY AND PROSPECTS

626   Aiming to improve mechanistic understanding of the relationship between the hydrogen-isotopic

627   signature of leaf waxes and the parent plants' source water, as required for reliable interpretation of

628     $\delta^2 H_{wax}$ as paleohydrological proxy in tropical East Africa, we compared $\delta^2 H_{wax}$ data obtained from

629   diverse species and growth forms of terrestrial plants in three distinct habitats around Lake Chala, and

630   during four successive seasons, with $\delta^2 H$ values of plant xylem and leaf water and of local precipitation.

631   All three basic parameters of *n*-alkane distribution (ACL, CPI, $C_{31}/(C_{29}+C_{31})$ ratio) as well as the

632   hydrogen-isotopic signatures of xylem water ($\delta^2 H_{xylem}$), *n*-alkanes ($\delta^2 H_{wax}$) and the biosynthetic

633   fractionation (ε_{bio}) varied with the general growth form of plants (grass, tree or shrub). The isotopic

signatures of δ^2H_{xylem}, δ^2H_{wax}, δ^2H_{leaf} and ε_{bio} also varied with habitat (lakeshore forest, crater rim, savanna), however this habitat effect is largely due to the fact that Lake Chala lakeshore vegetation 1) sources its water partly from lake water (cf. our data on *Thylacium africanum*), and 2) consists primarily of trees, whereas crater-rim and savanna vegetation consists mostly of grasses and shrubs.

Despite the evidence for seasonal trends in some subsets of our hydrogen-isotope data, season was never a significant driver of any tested variable. This result supports the findings presented by De Wispelaere et al. (2017) that the hydrology of the region's vegetation is dominated by a single water source (that is, besides evaporated lake water), notwithstanding receiving rainfall from two major and distinct monsoon systems. On the other hand, discriminating a distinct seasonal effect on plant hydrology in equatorial East Africa is complicated by the bimodality of its dry and rainy seasons, and substantial inter-annual variation in their expression. Resolution of this issue may thus have to await availability of seasonally well-resolved and high-volume datasets on (a few) individual plant species, preferably running over multiple years.

Finally, large portions of the variability in our hydrogen-isotope dataset can be explained by random species effects (at different levels, e.g. $\varepsilon_{leaf/xylem}$, $\varepsilon_{wax/leaf}$) which depend on intrinsic (plant phenological and biosynthesis-related) factors. Thus, for calibrating sedimentary δ^2H_{wax} signatures against vegetation it is crucial to obtain representative samples of all plant communities present within a study region.

Overall, our results show that in the Lake Chala region, source-water isotopic signatures surviving in plants' δ^2H_{wax} values are largely representative for precipitation falling during the short rainy season. This implies that paleohydrological studies in any region affected by multiple moisture sources should take into account possible bias in δ^2H_{wax} signatures due to unequal use of those moisture sources by the plants. Further, the strong influence of plant growth form on δ^2H_{wax} values should be taken into account, by directly juxtaposing sedimentary δ^2H_{wax} records against proxy information on temporal changes in plant community composition. Our results indicate that besides reconstructions of past vegetation change based on fossil pollen and fungal spores (e.g., van Geel et al., 2011) or the carbon-isotopic signatures of leaf-wax *n*-alkanes (e.g., Sinninghe Damsté et al., 2011) and grass pollen (e.g., Urban et al., 2015), also *n*-alkane distributions as reflected in the $C_{31}/(C_{29}+C_{31})$ ratio, ACL and CPI constitute potentially helpful proxies to trace changes in the dominant plant growth form present in the area. To their advantage, these proxies can be derived from the same *n*-alkane data sets employed to determine δ^2H_{wax}.

ACKNOWLEDGEMENTS

AUTHOR CONTRIBUTIONS

Field sampling was conducted by LDW and SB with botanical help from AH. Laboratory work was conducted by LDW and SB. Data analysis and interpretation was done by MG, LDW, MB, SB, DV and

673 PB. The manuscript was drafted by MG with input from DV and PB. All authors discussed the results
674 and contributed to the final manuscript.

675

676 **APPENDIX A. SUPPLEMENTARY MATERIAL**

677 Supplementary figures and data to this article can be found online at https://doi.org/10.1016/
678 j.gca.2019...

679 **REFERENCES**

680 Araguás-Araguás L., Rozanski K., Gonfiantini R. and Louvat D. (1995) Isotope effects accompanying
681 vacuum extraction of soil water for stable isotope analyses. *J. Hydrol.* **168**, 159–171.

682 Barker P. A., Hurrell E. R., Leng M. J., Wolff C., Cocquyt C., Sloane H. J. and Verschuren D. (2011)
683 Seasonality in equatorial climate over the past 25 k.y. revealed by oxygen isotope records from
684 Mount Kilimanjaro. *Geology* **39**, 1111–1114.

685 Bates D., Mächler M., Bolker B. and Walker S. (2015) Fitting linear mixed-effects models using lme4.
686 *J. Stat. Softw.* **67**, 1–48.

687 Berke M. A., Johnson T. C., Werne J. P., Grice K., Schouten S. and Sinninghe Damsté J. S. (2012)
688 Molecular records of climate variability and vegetation response since the Late Pleistocene in the
689 Lake Victoria basin, East Africa. *Quat. Sci. Rev.* **55**, 59–74.

690 Bray E. E. and Evans E. D. (1961) Distribution of n-paraffins as a clue to recognition of source beds.
691 *Geochim. Cosmochim. Acta* **22**, 2–15.

692 Buckles L. K., Weijers J. W. H., Verschuren D. and Sinninghe Damsté J. S. (2014) Sources of core and
693 intact branched tetraether membrane lipids in the lacustrine environment: Anatomy of Lake Challa
694 and its catchment, equatorial East Africa. *Geochim. Cosmochim. Acta* **140**, 106–126.

695 Bush R. T. and McInerney F. A. (2013) Leaf wax n-alkane distributions in and across modern plants:
696 Implications for paleoecology and chemotaxonomy. *Geochim. Cosmochim. Acta* **117**, 161–179.

697 Bush R. T. and McInerney F. A. (2015) Influence of temperature and C_4 abundance on n-alkane chain
698 length distributions across the central USA. *Org. Geochem.* **79**, 65–73.

699 Cernusak L. A., Barbour M. M., Arndt S. K., Cheesman A. W., English N. B., Feild T. S., Helliker B.
700 R., Holloway-Phillips M. M., Holtum J. A. M., Kahmen A., McInerney F. A., Munksgaard N. C.,
701 Simonin K. A., Song X., Stuart-Williams H., West J. B. and Farquhar G. D. (2016) Stable isotopes
702 in leaf water of terrestrial plants. *Plant Cell Environ.* **39**, 1087–1102.

703 Cernusak L. A., Pate J. S. and Farquhar G. D. (2002) Diurnal variation in the stable isotope composition
704 of water and dry matter in fruiting Lupinus angustifolius under field conditions. *Plant Cell Environ.*
705 **25**, 893–907.

706 Chikaraishi Y. and Naraoka H. (2007) $\delta^{13}C$ and δD relationships among three n-alkyl compound classes
707 (n-alkanoic acid, n-alkane and n-alkanol) of terrestrial higher plants. *Org. Geochem.* **38**, 198–215.

708   Clement A. C., Hall A. and Broccoli A. J. (2004) The importance of precessional signals in the tropical
709   climate. *Clim. Dyn.* **22**, 327–341.

710   Cormier M.-A., Werner R. A., Sauer P. E., Gröcke D. R., Leuenberger M. C., Wieloch T., Schleucher J.
711   and Kahmen A. (2018) ^{2}H-fractionations during the biosynthesis of carbohydrates and lipids imprint
712   a metabolic signal on the δ^2H values of plant organic compounds. *New Phytol.* **218**, 479–491.

713   Costa K., Russell J., Konecky B. and Lamb H. (2014) Isotopic reconstruction of the African Humid
714   Period and Congo Air Boundary migration at Lake Tana, Ethiopia. *Quat. Sci. Rev.* **83**, 58–67.

715   Craig H. (1961) Isotopic variations in meteoric waters. *Science* **133**, 1702–1703.

716   Dansgaard W. (1964) Stable isotopes in precipitation. *Tellus* **16**, 436–468.

717   Dawson T. E. and Ehleringer J. R. (1991) Streamside trees that do not use stream water. *Nature* **350**,
718   335–337.

719   De Wispelaere L., Bodé S., Hervé-Fernández P., Hemp A., Verschuren D. and Boeckx P. (2017) Plant
720   water resource partitioning and isotopic fractionation during transpiration in a seasonally dry tropical
721   climate. *Biogeosciences* **14**, 73–88.

722   Diefendorf A. F., Freeman K. H., Wing S. L. and Graham H. V. (2011) Production of n-alkyl lipids in
723   living plants and implications for the geologic past. *Geochim. Cosmochim. Acta* **75**, 7472–7485.

724   Diefendorf A. F. and Freimuth E. J. (2017) Extracting the most from terrestrial plant-derived n-alkyl
725   lipids and their carbon isotopes from the sedimentary record: A review. *Org. Geochem.* **103**, 1–21.

726   Douglas P. M., Pagani M., Eglinton T. I., Brenner M., Hodell D. A., Curtis J. H., Ma K. F. and
727   Breckenridge A. (2014) Pre-aged plant waxes in tropical lake sediments and their influence on the
728   chronology of molecular paleoclimate proxy records. *Geochim. Cosmochim. Acta* **141**, 346–364.

729   Eglinton G. and Hamilton R. J. (1967) Leaf epicuticular waxes. *Science* **156**, 1322–1335.

730   Eglinton T. I. and Eglinton G. (2008) Molecular proxies for paleoclimatology. *Earth Planet. Sci. Lett.*
731   **275**, 1–16.

732   Eley Y., Dawson L., Black S., Andrews J. and Pedentchouk N. (2014) Understanding ^{2}H/^{1}H systematics
733   of leaf wax n-alkanes in coastal plants at Stiffkey saltmarsh, Norfolk, UK. *Geochim. Cosmochim.*
734   *Acta* **128**, 13–28.

735   Ellsworth P. Z. and Williams D. G. (2007) Hydrogen isotope fractionation during water uptake by woody
736   xerophytes. *Plant Soil* **291**, 93–107.

737   Evaristo J., Jasechko S. and McDonnell J. J. (2015) Global separation of plant transpiration from
738   groundwater and streamflow. *Nature* **525**, 91–94.

739   Feakins S. J., Bentley L. P., Salinas N., Shenkin A., Blonder B., Goldsmith G. R., Ponton C., Arvin L.
740   J., Wu M. S., Peters T., West A. J., Martin R. E., Enquist B. J., Asner G. P. and Malhi Y. (2016)
741   Plant leaf wax biomarkers capture gradients in hydrogen isotopes of precipitation from the Andes
742   and Amazon. *Geochim. Cosmochim. Acta* **182**, 155–172.

743 Feakins S. J. and Sessions A. L. (2010) Controls on the D/H ratios of plant leaf waxes in an arid
744 ecosystem. *Geochim. Cosmochim. Acta* **74**, 2128–2141.

745 Feakins S. J., Wu M. S., Ponton C., Galy V. and West A. J. (2018) Dual isotope evidence for sedimentary
746 integration of plant wax biomarkers across an Andes-Amazon elevation transect. *Geochim.*
747 *Cosmochim. Acta* **242**, 64–81.

748 Freeman K. H. and Pancost R. D. (2014) Biomarkers for terrestrial plants and climate. *Treatise Geochem.*
749 **12**, 395–416.

750 Gao L., Edwards E. J., Zeng Y. and Huang Y. (2014) Major evolutionary trends in hydrogen isotope
751 fractionation of vascular plant leaf waxes. *PLoS ONE* **9**, e112610.

752 Garcin Y., Deschamps P., Ménot G., Saulieu G. de, Schefuß E., Sebag D., Dupont L. M., Oslisly R.,
753 Brademann B., Mbusnum K. G., Onana J.-M., Ako A. A., Epp L. S., Tjallingii R., Strecker M. R.,
754 Brauer A. and Sachse D. (2018) Early anthropogenic impact on Western Central African rainforests
755 2,600 y ago. *Proc. Natl. Acad. Sci.* **115**, 3261–3266.

756 Garcin Y., Schwab V. F., Gleixner G., Kahmen A., Todou G., Séné O., Onana J.-M., Achoundong G.
757 and Sachse D. (2012) Hydrogen isotope ratios of lacustrine sedimentary n-alkanes as proxies of
758 tropical African hydrology: Insights from a calibration transect across Cameroon. *Geochim.*
759 *Cosmochim. Acta* **79**, 106–126.

760 Gat J. R. (2010) Isotope hydrology: A study of the water cycle. Imperial College Press, London, UK.

761 Gat J. R. (1996) Oxygen and hydrogen isotopes in the hydrological cycle. *Annu. Rev. Earth Planet. Sci.*
762 **24**, 225–262.

763 van Geel B., Gelorini V., Lyaruu A., Aptroot A., Rucina S., Marchant R., Damsté J. S. S. and Verschuren
764 D. (2011) Diversity and ecology of tropical African fungal spores from a 25,000-year
765 palaeoenvironmental record in southeastern Kenya. *Rev. Palaeobot. Palynol.* **164**, 174–190.

766 Griepentrog M., Bodé S., Boeckx P. and Wiesenberg G. L. B. (2016) The fate of plant wax lipids in a
767 model forest ecosystem under elevated CO_2 concentration and increased nitrogen deposition. *Org.*
768 *Geochem.* **98**, 131–140.

769 Helliker B. R. and Ehleringer J. R. (2000) Establishing a grassland signature in veins: ^{18}O in the leaf
770 water of C_3 and C_4 grasses. *Proc. Natl. Acad. Sci.* **97**, 7894–7898.

771 Hemp A. (2006) Vegetation of Kilimanjaro: hidden endemics and missing bamboo. *Afr. J. Ecol.* **44**, 305–
772 328.

773 Hou J., D'Andrea W. J. and Huang Y. (2008) Can sedimentary leaf waxes record D/H ratios of
774 continental precipitation? Field, model, and experimental assessments. *Geochim. Cosmochim. Acta*
775 **72**, 3503–3517.

776 Jansen B., Haussmann N. S., Tonneijck F. H., Verstraten J. M. and de Voogt P. (2008) Characteristic
777 straight-chain lipid ratios as a quick method to assess past forest–páramo transitions in the
778 Ecuadorian Andes. *Palaeogeogr. Palaeoclimatol. Palaeoecol.* **262**, 129–139.

Kahmen A., Hoffmann B., Schefuß E., Arndt S. K., Cernusak L. A., West J. B. and Sachse D. (2013) Leaf water deuterium enrichment shapes leaf wax n-alkane δD values of angiosperm plants II: Observational evidence and global implications. *Geochim. Cosmochim. Acta* **111**, 50–63.

Kahmen A., Simonin K., Tu K. P., Merchant A., Callister A., Siegwolf R., Dawson T. E. and Arndt S. K. (2008) Effects of environmental parameters, leaf physiological properties and leaf water relations on leaf water $\delta^{18}O$ enrichment in different Eucalyptus species. *Plant Cell Environ.* **31**, 738–751.

Li S.-G., Tsujimura M., Sugimoto A., Sasaki L., Yamanaka T., Davaa G., Oyunbaatar D. and Sugita M. (2006) Seasonal variation in oxygen isotope composition of waters for a montane larch forest in Mongolia. *Trees* **20**, 122–130.

Liu J., Liu W., An Z. and Yang H. (2016) Different hydrogen isotope fractionations during lipid formation in higher plants: Implications for paleohydrology reconstruction at a global scale. *Sci. Rep.* **6**, 19711.

Liu W. and Yang H. (2008) Multiple controls for the variability of hydrogen isotopic compositions in higher plant n-alkanes from modern ecosystems. *Glob. Change Biol.* **14**, 2166–2177.

Mallard, G. (2014). AMDIS – Developing Libraries. *National Institute of Standards and Technology.* Retrieved from https://blog.sepscience.com/massspectrometry/ms-solutions-23-amdis-developing-libraries (on 16th June 2019).

Martín-Gómez P., Barbeta A., Voltas J., Peñuelas J., Dennis K., Palacio S., Dawson T. E. and Ferrio J. P. (2015) Isotope-ratio infrared spectroscopy: a reliable tool for the investigation of plant-water sources? *New Phytol.* **207**, 914–927.

McInerney F. A., Helliker B. R. and Freeman K. H. (2011) Hydrogen isotope ratios of leaf wax n-alkanes in grasses are insensitive to transpiration. *Geochim. Cosmochim. Acta* **75**, 541–554.

Meier-Augenstein W. and Schimmelmann A. (2019) A guide for proper utilisation of stable isotope reference materials. *Isotopes Environ. Health Stud.* **55**, 113–128.

Moernaut J., Verschuren D., Charlet F., Kristen I., Fagot M. and De Batist M. (2010) The seismic-stratigraphic record of lake-level fluctuations in Lake Challa: Hydrological stability and change in equatorial East Africa over the last 140kyr. *Earth Planet. Sci. Lett.* **290**, 214–223.

Nakagawa S. and Schielzeth H. (2013) A general and simple method for obtaining R2 from generalized linear mixed-effects models. *Methods Ecol. Evol.* **4**, 133–142.

Nelson D. B., Ladd S. N., Schubert C. J. and Kahmen A. (2018) Rapid atmospheric transport and large-scale deposition of recently synthesized plant waxes. *Geochim. Cosmochim. Acta* **222**, 599–617.

Newberry S. L., Kahmen A., Dennis P. and Grant A. (2015) n-Alkane biosynthetic hydrogen isotope fractionation is not constant throughout the growing season in the riparian tree *Salix viminalis*. *Geochim. Cosmochim. Acta* **165**, 75–85.

Nicholson S. E. (2018) The ITCZ and the seasonal cycle over equatorial Africa. *Bull. Am. Meteorol. Soc.* **99**, 337–348.

815 Nicholson S. E. (2000) The nature of rainfall variability over Africa on time scales of decades to millenia.
816 *Glob. Planet. Change* **26**, 137–158.

817 Payne B. R. (1970) Water balance of Lake Chala and its relation to groundwater from tritium and stable
818 isotope data. *J. Hydrol.* **11**, 47–58.

819 Poca M., Coomans O., Urcelay C., Zeballos S. R., Bodé S. and Boeckx P. (2019) Isotope fractionation
820 during root water uptake by *Acacia caven* is enhanced by arbuscular mycorrhizas. *Plant Soil*.
821 https://doi.org/10.1007/s11104-019-04139-1.

822 Polissar P. J. and Freeman K. H. (2010) Effects of aridity and vegetation on plant-wax δD in modern
823 lake sediments. *Geochim. Cosmochim. Acta* **74**, 5785–5797.

824 R Core Team (2018) R: A language and environment for statistical computing. Available at:
825 http://www.R-project.org.

826 Rieley G., Collier R. J., Jones D. M. and Eglinton G. (1991) The biogeochemistry of Ellesmere Lake,
827 U.K.—I: source correlation of leaf wax inputs to the sedimentary lipid record. *Org. Geochem.* **17**,
828 901–912.

829 Rommerskirchen F., Plader A., Eglinton G., Chikaraishi Y. and Rullkötter J. (2006) Chemotaxonomic
830 significance of distribution and stable carbon isotopic composition of long-chain alkanes and alkan-
831 1-ols in C4 grass waxes. *Org. Geochem.* **37**, 1303–1332.

832 Sachse D., Billault I., Bowen G. J., Chikaraishi Y., Dawson T. E., Feakins S. J., Freeman K. H., Magill
833 C. R., McInerney F. A., van der Meer M. T. J., Polissar P., Robins R. J., Sachs J. P., Schmidt H.-L.,
834 Sessions A. L., White J. W. C., West J. B. and Kahmen A. (2012) Molecular paleohydrology:
835 interpreting the hydrogen-isotopic composition of lipid biomarkers from photosynthesizing
836 organisms. *Annu. Rev. Earth Planet. Sci.* **40**, 221–249.

837 Sachse D., Radke J. and Gleixner G. (2004) Hydrogen isotope ratios of recent lacustrine sedimentary n-
838 alkanes record modern climate variability. *Geochim. Cosmochim. Acta* **68**, 4877–4889.

839 Schefuß E., Schouten S. and Schneider R. R. (2005) Climatic controls on central African hydrology
840 during the past 20,000 years. *Nature* **437**, 1003–1006.

841 Schimmelmann A., Lewan M. D. and Wintsch R. P. (1999) D/H isotope ratios of kerogen, bitumen, oil,
842 and water in hydrous pyrolysis of source rocks containing kerogen types I, II, IIS, and III. *Geochim.*
843 *Cosmochim. Acta* **63**, 3751–3766.

844 Schneider T., Bischoff T. and Haug G. H. (2014) Migrations and dynamics of the intertropical
845 convergence zone. *Nature* **513**, 45–53.

846 Sessions A. L. (2016) Factors controlling the deuterium contents of sedimentary hydrocarbons. *Org.*
847 *Geochem.* **96**, 43–64.

848 Sessions A. L. (2006) Seasonal changes in D/H fractionation accompanying lipid biosynthesis in
849 *Spartina alterniflora*. *Geochim. Cosmochim. Acta* **70**, 2153–2162.

850 Sessions A. L., Burgoyne T. W., Schimmelmann A. and Hayes J. M. (1999) Fractionation of hydrogen
851 isotopes in lipid biosynthesis. *Org. Geochem.* **30**, 1193–1200.

852 Shepherd T. and Griffiths D. W. (2006) The effects of stress on plant cuticular waxes. *New Phytol.* **171**,
853   469–499.

854 Sinninghe Damsté J. S., Verschuren D., Ossebaar J., Blokker J., van Houten R., van der Meer M. T. J.,
855   Plessen B. and Schouten S. (2011) A 25,000-year record of climate-induced changes in lowland
856   vegetation of eastern equatorial Africa revealed by the stable carbon-isotopic composition of fossil
857   plant leaf waxes. *Earth Planet. Sci. Lett.* **302**, 236–246.

858 Smith F. A. and Freeman K. H. (2006) Influence of physiology and climate on δD of leaf wax n-alkanes
859   from C_3 and C_4 grasses. *Geochim. Cosmochim. Acta* **70**, 1172–1187.

860 Tierney J. E., Russell J. M., Huang Y., Damsté J. S. S., Hopmans E. C. and Cohen A. S. (2008) Northern
861   hemisphere controls on tropical southeast African climate during the past 60,000 Years. *Science* **322**,
862   252–255.

863 Tierney J. E., Russell J. M., Sinninghe Damsté J. S., Huang Y. and Verschuren D. (2011) Late Quaternary
864   behavior of the East African monsoon and the importance of the Congo Air Boundary. *Quat. Sci.*
865   *Rev.* **30**, 798–807.

866 Urban M. A., Nelson D. M., Street-Perrott F. A., Verschuren D. and Hu F. S. (2015) A late-Quaternary
867   perspective on atmospheric pCO_2, climate, and fire as drivers of C_4-grass abundance. *Ecology* **96**,
868   642–653.

869 Verschuren D., Sinninghe Damsté J. S., Moernaut J., Kristen I., Blaauw M., Fagot M., Haug G. H., Geel
870   B. van, Batist M. D., Barker P., Vuille M., Conley D. J., Olago D. O., Milne I., Plessen B., Eggermont
871   H., Wolff C., Hurrell E., Ossebaar J., Lyaruu A., Plicht J. van der, Cumming B. F., Brauer A., Rucina
872   S. M., Russell J. M., Keppens E., Hus J., Bradley R. S., Leng M., Mingram J. and Nowaczyk N. R.
873   (2009) Half-precessional dynamics of monsoon rainfall near the East African Equator. *Nature* **462**,
874   637–641.

875 Vogts A., Moossen H., Rommerskirchen F. and Rullkötter J. (2009) Distribution patterns and stable
876   carbon isotopic composition of alkanes and alkan-1-ols from plant waxes of African rain forest and
877   savanna C_3 species. *Org. Geochem.* **40**, 1037–1054.

878 West A. G., Patrickson S. J. and Ehleringer J. R. (2006) Water extraction times for plant and soil materials
879   used in stable isotope analysis. *Rapid Commun. Mass Spectrom.* **20**, 1317–1321.

880 White J. W. C., Cook E. R., Lawrence J. R. and Wallace S. B. (1985) The D/H ratios of sap in trees:
881   Implications for water sources and tree ring D/H ratios. *Geochim. Cosmochim. Acta* **49**, 237–246.

882 Zech M., Leiber K., Zech W., Poetsch T. and Hemp A. (2011) Late Quaternary soil genesis and
883   vegetation history on the northern slopes of Mt. Kilimanjaro, East Africa. *Quat. Int.* **243**, 327–336.

884 Zhao L., Wang L., Cernusak L. A., Liu X., Xiao H., Zhou M. and Zhang S. (2016) Significant
885   difference in hydrogen isotope composition between xylem and tissue water in *Populus*
886   *euphratica*. *Plant Cell Environ.* **39**, 1848–1857.

Fig. 1.   Aerial view of the Lake Chala crater rim, bridging the border between Kenya and Tanzania in equatorial East Africa, with vegetation sampling locations in the three principal local habitats (crater rim, lakeshore, savanna).

Fig. 2.   Carbon preference index (CPI) representing the odd-over-even predominance of *n*-alkane carbon chain lengths (C_{27}-C_{33}) in leaves of different plant growth forms (panels: grasses, shrubs, trees) sampled at different seasons (shades of grey: short dry, SE monsoon, long dry, NE monsoon) and averaged across different habitats. Here and in all further box-plot figures, the boxes show the median value (thick line) and the first and third quartiles (25th and 75th percentiles), the whiskers represent 1.5 times the interquartile (IQR) range, and isolated dots represent outliers beyond 1.5 IQR.

Fig. 3.   The ratio of *n*-alkane carbon chain lengths $C_{31}/(C_{29}+C_{31})$ in leaves of different plant growth forms (grasses, shrubs, trees) and averaged across different habitats and seasons.

Fig. 4.   Abundance-weighted mean hydrogen-isotopic signature of C_{29} and C_{31} *n*-alkanes (δ^2H_{wax}) in leaves among 14 plant species of various growth form (shades of grey: grass, shrub, tree) sampled in three habitats (from top to bottom: crater rim, lakeshore, savanna) and averaged across seasons, with *n* representing the number of observations.

Fig. 5.   Hydrogen-isotopic signature of xylem water (δ^2H_{xylem}) among 12 plant species of various growth form (shades of grey: shrub, tree) sampled in three habitats (from top to bottom: crater rim, lakeshore, savanna) and averaged across seasons, with *n* representing the number of observations.

Fig. 6.   Hydrogen-isotopic signature of leaf water (δ^2H_{leaf}) among 14 plant species of various growth form (shades of grey: grass, shrub, tree) sampled in three habitats (from top to bottom: crater rim, lakeshore, savanna) and averaged across seasons, with *n* representing the number of observations.
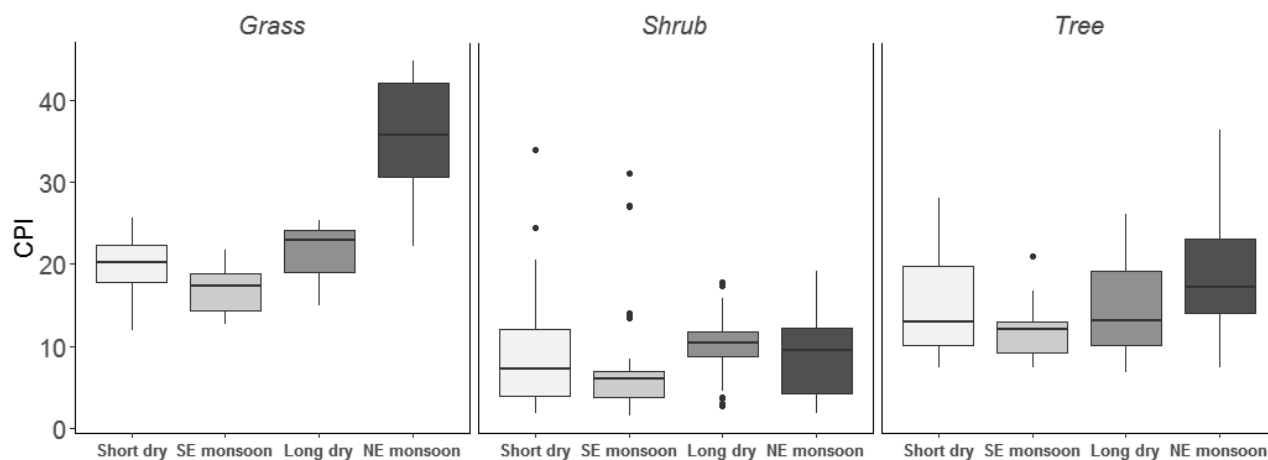
Fig. 7.   Biosynthetic fractionation (ε_{bio}, i.e. $\varepsilon_{wax/leaf}$) between the hydrogen-isotopic signature of leaf water (δ^2H_{leaf}) and the abundance-weighted mean hydrogen-isotopic signature of C_{29} and C_{31} *n*-alkanes (δ^2H_{wax}), among 14 plant species of various growth form (shades of grey: grass, shrub, tree) sampled in three habitats (from top to bottom: crater rim, lakeshore, savanna) and averaged across seasons, with *n* representing the number of observations.

Fig. 8.   Conceptual scheme (modified after Sachse et al., 2012) showing the hydrogen-isotopic signatures (δ^2H) of different water pools (source water, leaf water) and of leaf-wax *n*-alkanes (δ^2H_{wax}) as well as the hydrogen-isotopic enrichment ($\varepsilon_{a/b}$) between different products (a) and sources (b) in the Lake Chala area. $\varepsilon_{leaf/source}$: enrichment between source water and leaf water due to evapotranspiration and possibly root water uptake; ε_{bio} (= $\varepsilon_{wax/leaf}$): enrichment between leaf water and leaf-wax *n*-alkanes due to biosynthetic fractionation; ε_{net} (= $\varepsilon_{wax/source}$): enrichment between source water and leaf-wax *n*-alkanes. Values represent overall averages across all plant species, habitats and seasons along with the standard deviation and the number of observations (*n*). The source water is either volume-weighted annual-average and NE monsoon precipitation or xylem water (De Wispelaere et al., 2017). Since there is no

923   xylem water data available for grasses, all $\varepsilon_{leaf/source}$ and ε_{net} values were calculated excluding grasses for

924   comparison. The sizes of arrows and boxes are only for conceptual representation and not scaled to actual
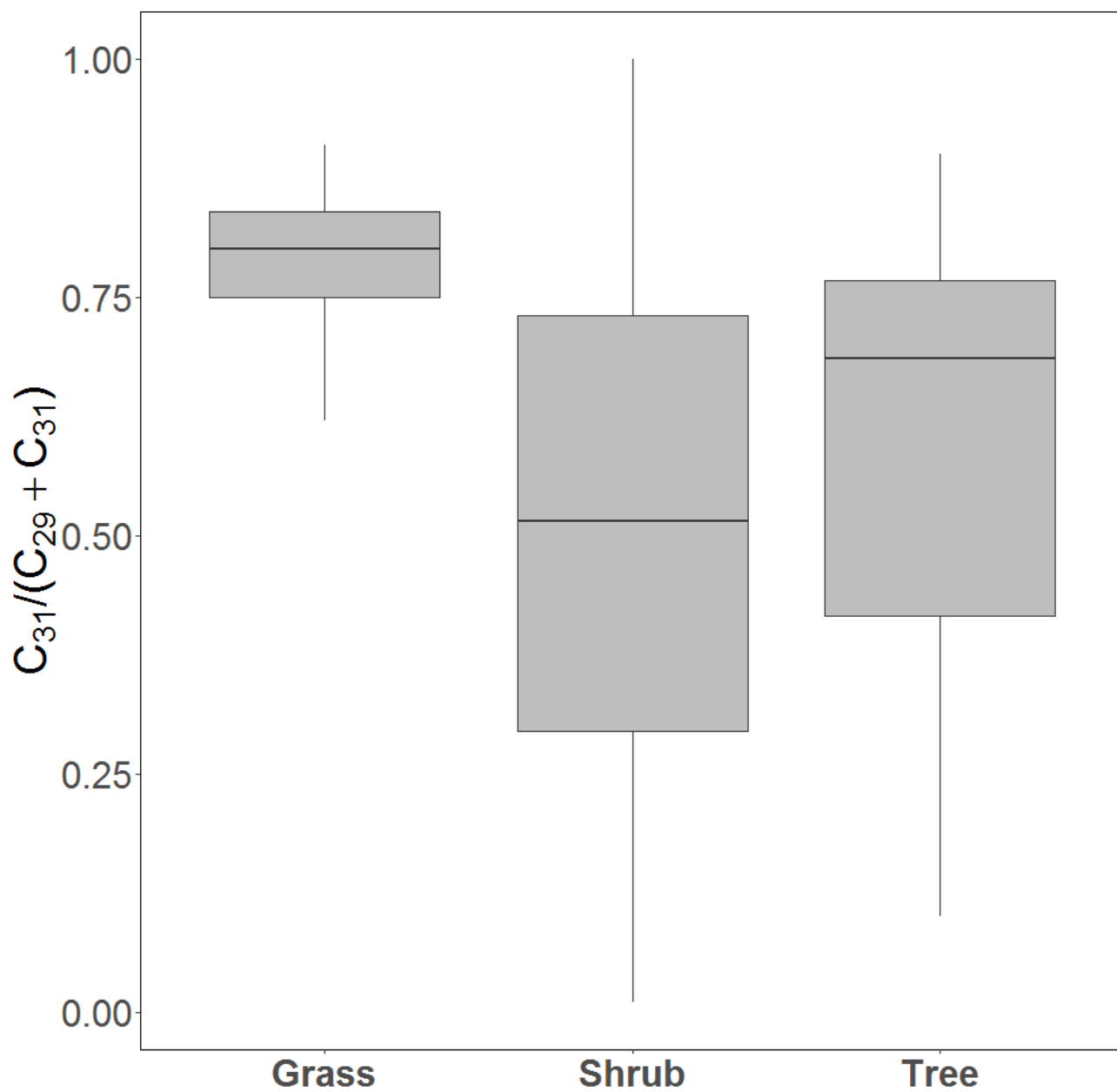
925   values.

FIGURES
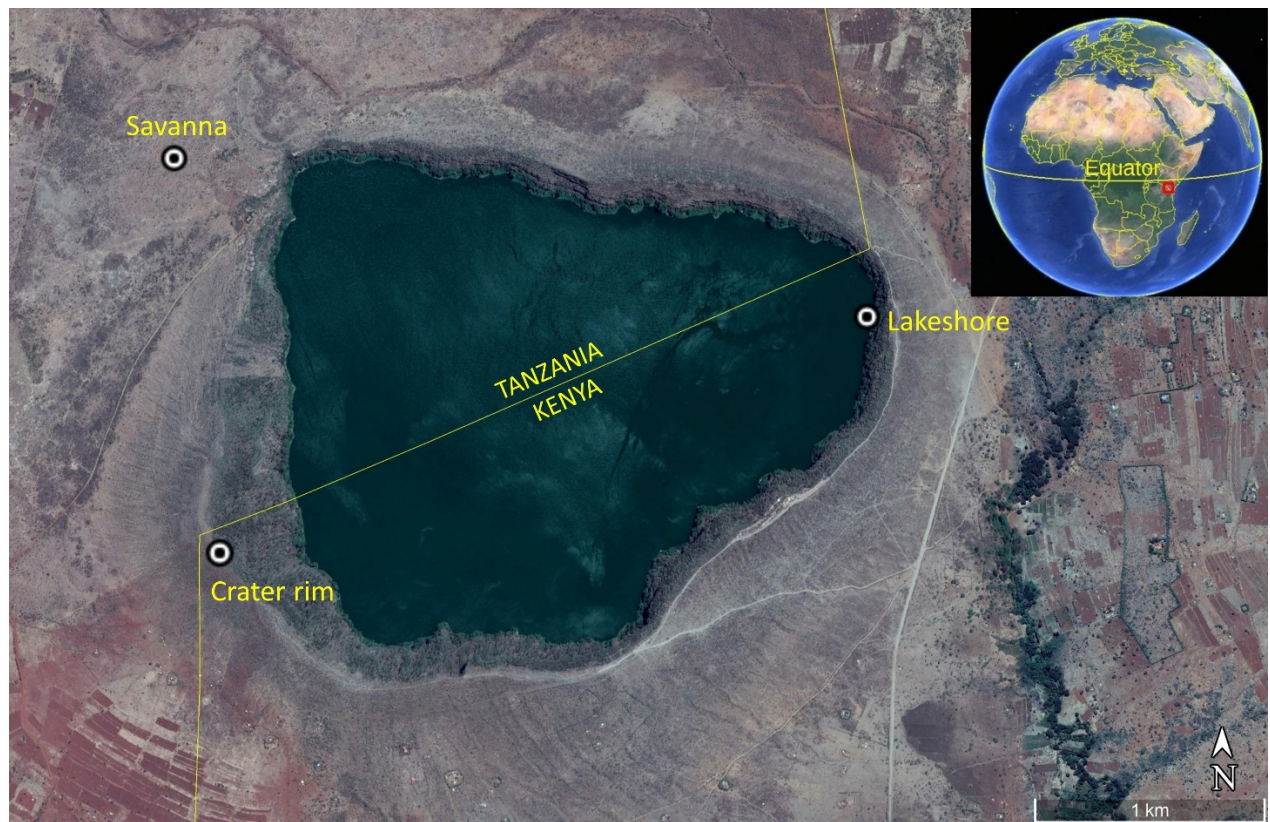
928 **Fig. 1.** Aerial view of the Lake Chala crater rim, bridging the border between Kenya and Tanzania in
929 equatorial East Africa, with vegetation sampling locations in the three principal local habitats (crater rim,
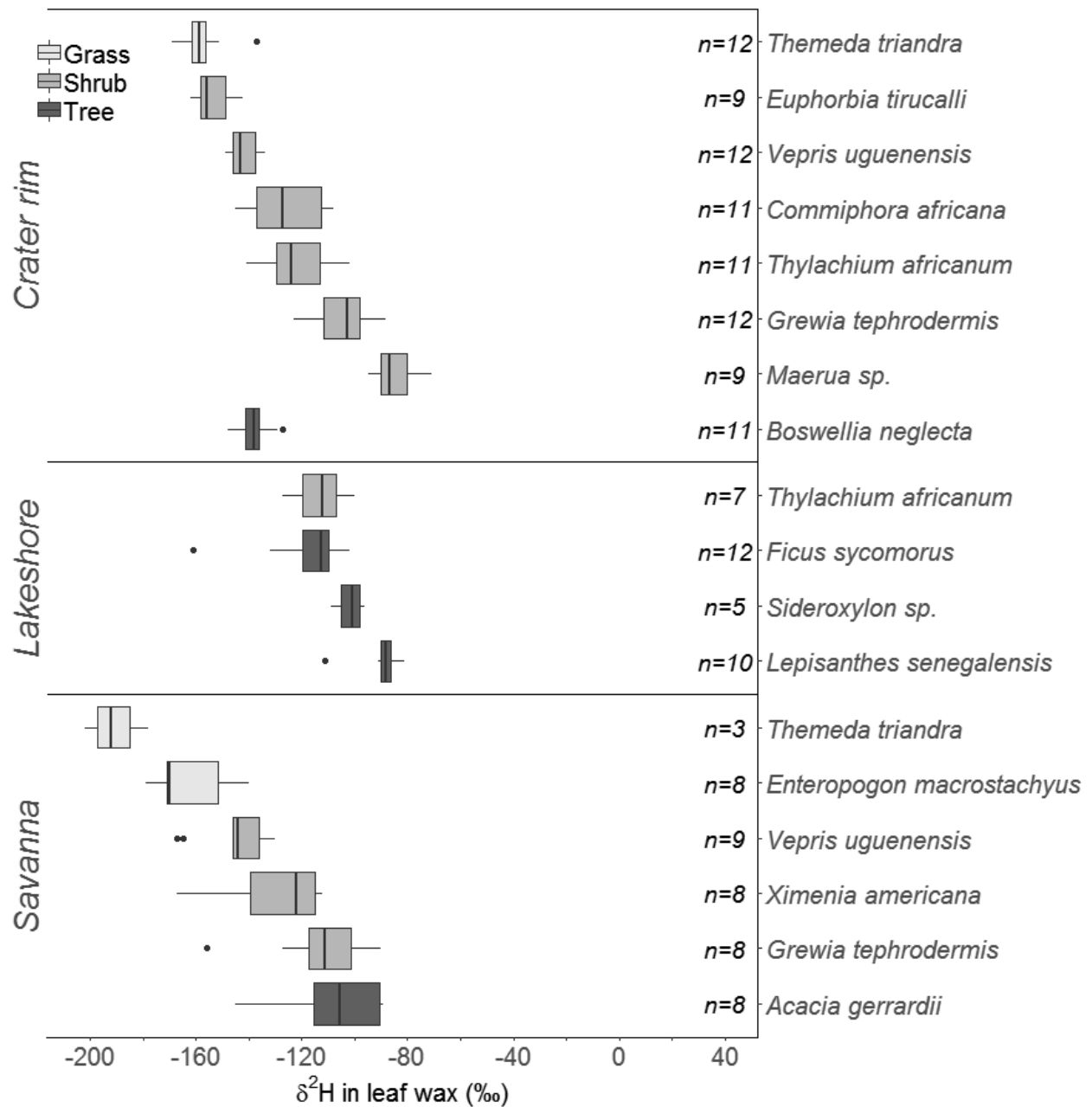930 lakeshore, savanna).

931

Fig. 2. Carbon preference index (CPI) representing the odd-over-even predominance of *n*-alkane carbon chain lengths (C_{27}-C_{33}) in leaves of different plant growth forms (panels: grasses, shrubs, trees) sampled at different seasons (shades of grey: short dry, SE monsoon, long dry, NE monsoon) and averaged across different habitats. Here and in all further box-plot figures, the boxes show the median value (thick line) and the first and third quartiles (25th and 75th percentiles), the whiskers represent 1.5 times the interquartile (IQR) range, and isolated dots represent outliers beyond 1.5 IQR.
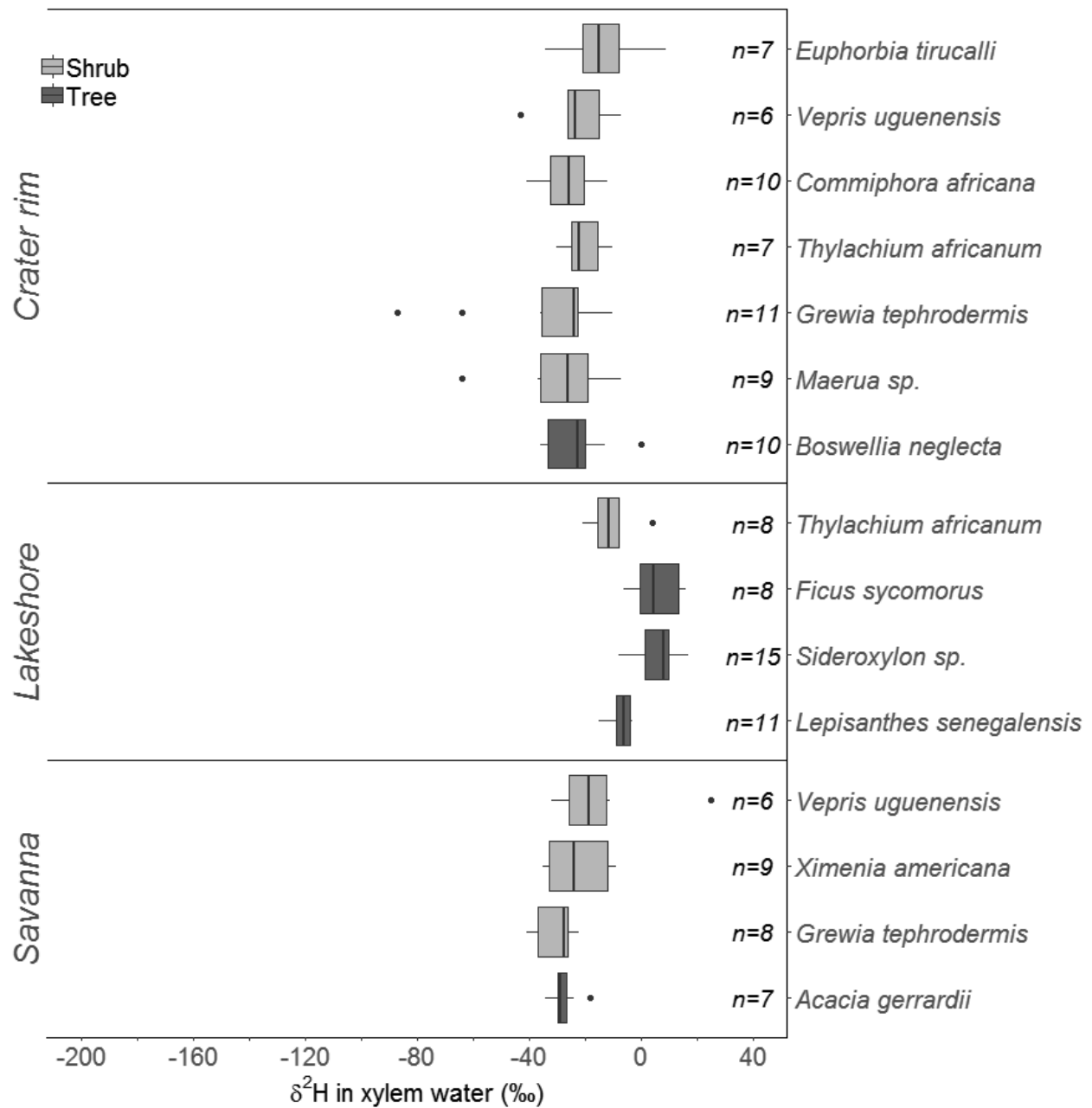
938

Fig. 3. The ratio of *n*-alkane carbon chain lengths $C_{31}/(C_{29}+C_{31})$ in leaves of different plant growth forms (grasses, shrubs, trees) and averaged across different habitats and seasons.
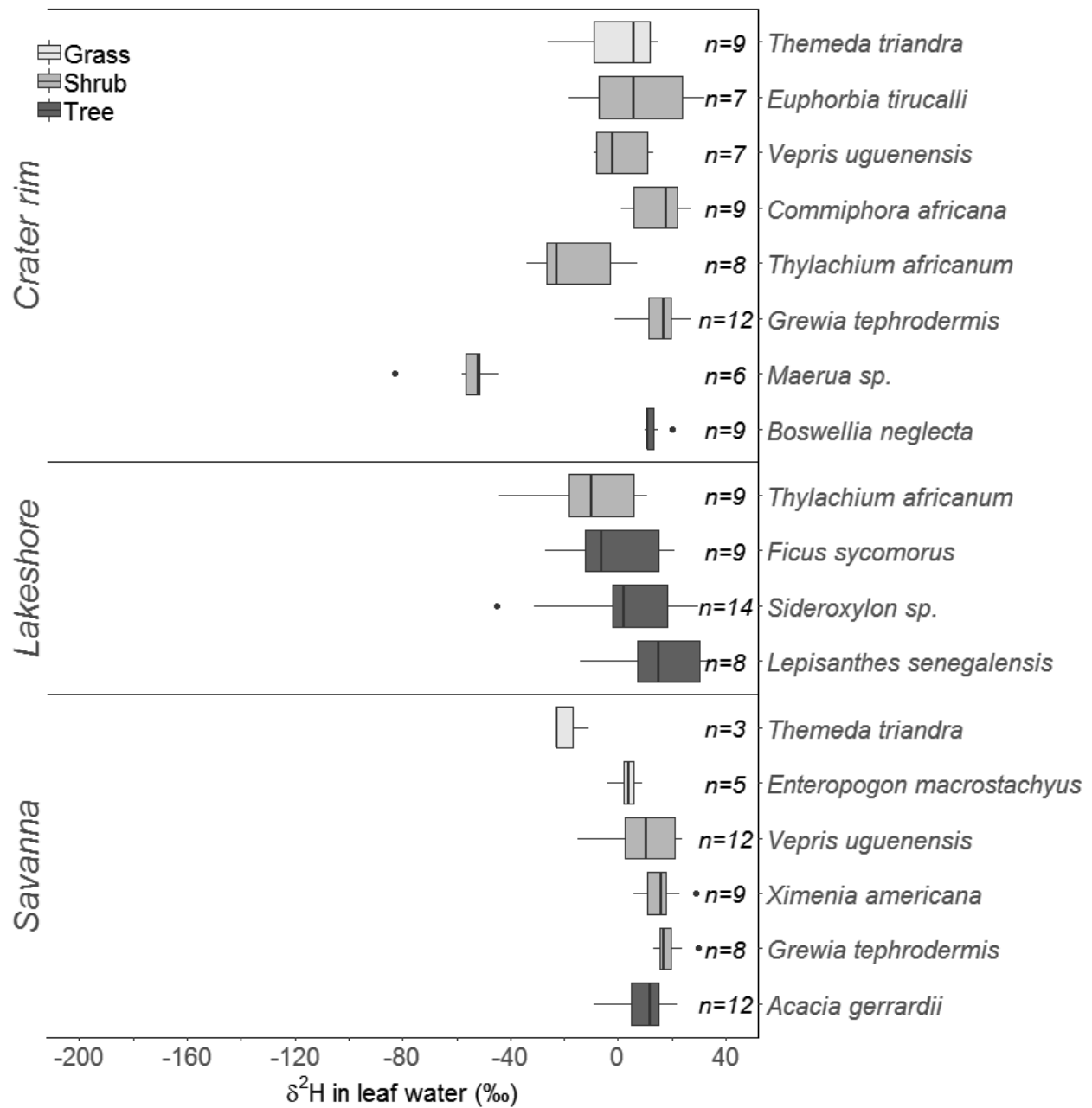
Fig. 4. Abundance-weighted mean hydrogen-isotopic signature of C_{29} and C_{31} *n*-alkanes (δ^2H_{wax}) in leaves among 14 plant species of various growth form (shades of grey: grass, shrub, tree) sampled in three habitats (from top to bottom: crater rim, lakeshore, savanna) and averaged across seasons, with *n* representing the number of observations.

946

Fig. 5. Hydrogen-isotopic signature of xylem water (δ^2H_{xylem}) among 12 plant species of various
growth form (shades of grey: shrub, tree) sampled in three habitats (from top to bottom: crater rim,
lakeshore, savanna) and averaged across seasons, with *n* representing the number of observations.

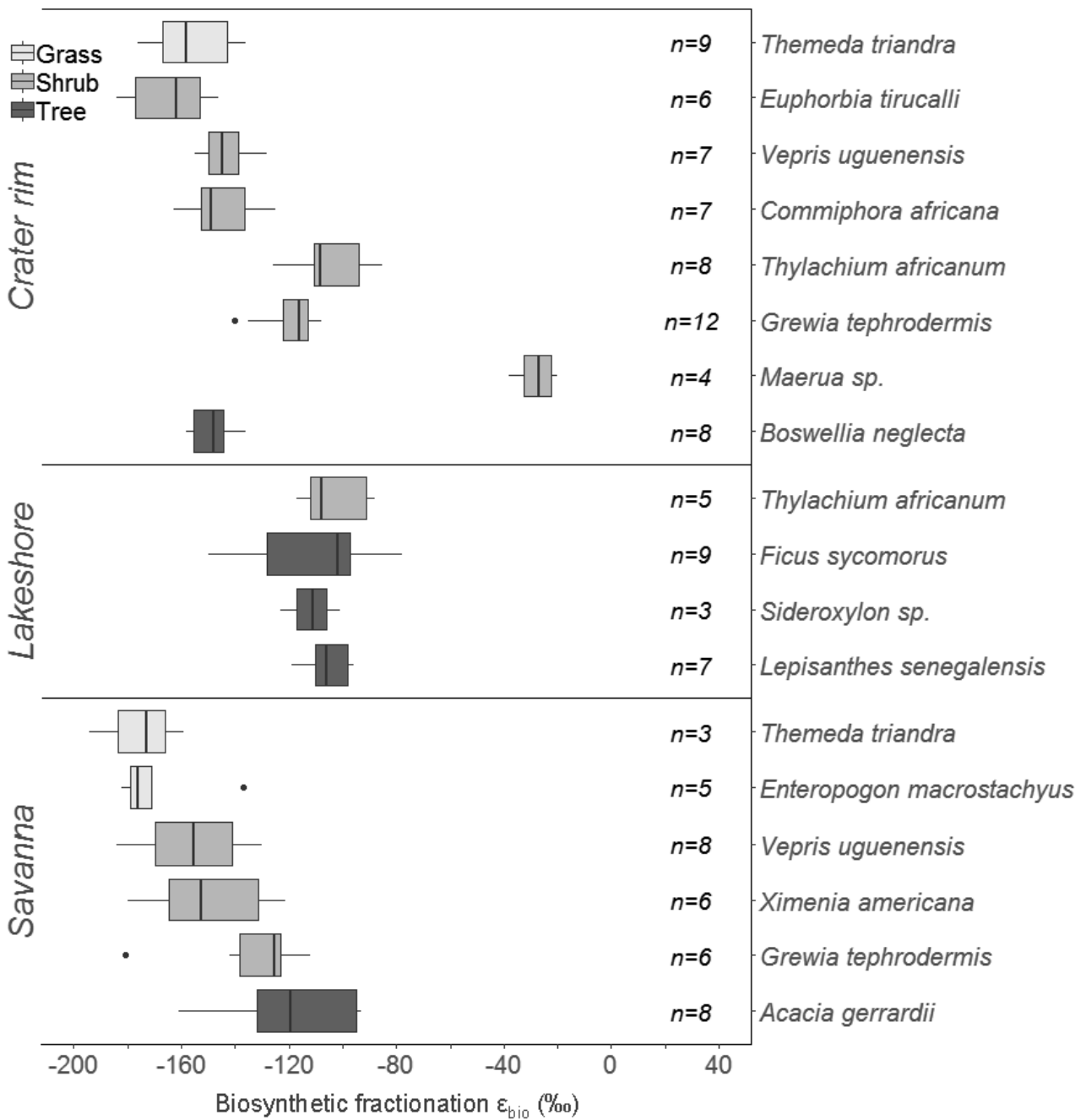950

Fig. 6. Hydrogen-isotopic signature of leaf water (δ^2H_{leaf}) among 14 plant species of various growth form (shades of grey: grass, shrub, tree) sampled in three habitats (from top to bottom: crater rim, lakeshore, savanna) and averaged across seasons, with *n* representing the number of observations.

Fig. 7. Biosynthetic fractionation (ε_{bio}, i.e. $\varepsilon_{wax/leaf}$) between the hydrogen-isotopic signature of leaf water (δ^2H_{leaf}) and the abundance-weighted mean hydrogen-isotopic signature of C_{29} and C_{31} n-alkanes (δ^2H_{wax}), among 14 plant species of various growth form (shades of grey: grass, shrub, tree) sampled in three habitats (from top to bottom: crater rim, lakeshore, savanna) and averaged across seasons, with n representing the number of observations.
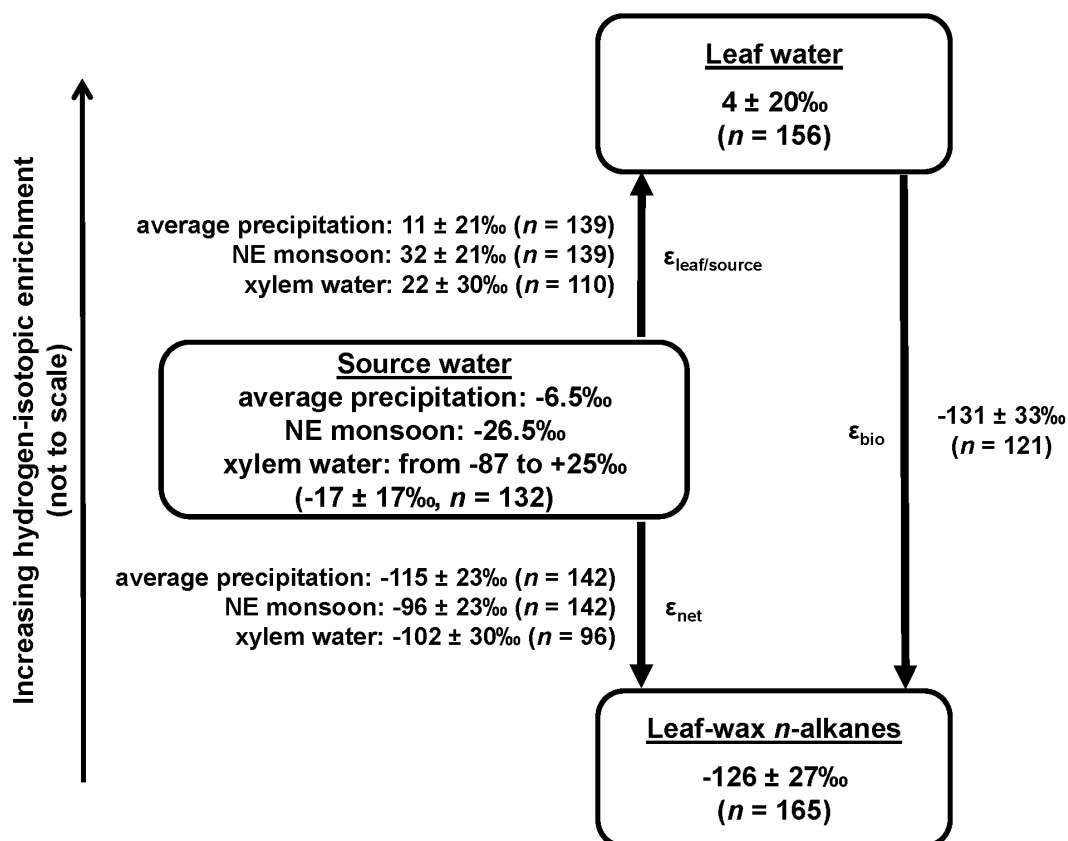
960

Fig. 8. Conceptual scheme (modified after Sachse et al., 2012) showing the hydrogen-isotopic signatures ($\delta^2 H$) of different water pools (source water, leaf water) and of leaf-wax n-alkanes ($\delta^2 H_{wax}$) as well as the hydrogen-isotopic enrichment ($\varepsilon_{a/b}$) between different products (a) and sources (b) in the Lake Chala area. $\varepsilon_{leaf/source}$: enrichment between source water and leaf water due to evapotranspiration and possibly root water uptake; ε_{bio} (= $\varepsilon_{wax/leaf}$): enrichment between leaf water and leaf-wax n-alkanes due to biosynthetic fractionation; ε_{net} (= $\varepsilon_{wax/source}$): enrichment between source water and leaf-wax n-alkanes. Values represent overall averages across all plant species, habitats and seasons along with the standard deviation and the number of observations (n). The source water is either volume-weighted annual-average and NE monsoon precipitation or xylem water (De Wispelaere et al., 2017). Since there is no xylem water data available for grasses, all $\varepsilon_{leaf/source}$ and ε_{net} values were calculated excluding grasses for comparison. The sizes of arrows and boxes are only for conceptual representation and not scaled to actual values.

TABLE CAPTIONS

974 **Table 1** Plant species and family with their respective growth form (grass, shrub, tree) and habitat (crater
975 rim, lakeshore, savanna).

976 **Table 2** Output of linear mixed-effect models for average chain length (ACL), carbon preference index
977 (CPI), the ratio of n-alkane carbon chain lengths $C_{31}/(C_{29}+C_{31})$, abundance-weighted mean hydrogen-
978 isotopic signature of C_{29} and C_{31} n-alkanes (δ^2H_{wax}), the hydrogen-isotopic signature of leaf water
979 (δ^2H_{leaf}), and biosynthetic enrichment (ε_{bio}) between δ^2H_{leaf} and δ^2H_{wax} as target variables, and with
980 growth form (grass, shrub, tree), habitat (crater rim, lakeshore, savanna) and season (long dry, NE
981 monsoon, SE monsoon, short dry) as fixed effects and species as random effect. The reference treatment
982 were grasses at the crater rim during the long dry season.

984 **Table 1**

985 Plant species and family with their respective growth form (grass, shrub, tree) and habitat (crater rim,

986 lakeshore, savanna).

Plant species	Plant family	Growth form	Habitat
Enteropogon macrostachyus	Poaceae	Grass	Savanna
Themeda triandra	Poaceae	Grass	Crater rim + Savanna
Commiphora africana	Burseraceae	Shrub	Crater rim
Grewia tephrodermis	Tiliaceae	Shrub	Crater rim + Savanna
Euphorbia tirucalli	Euphorbiaceae	Shrub	Crater rim
Maerua sp.	Capparaceae	Shrub	Crater rim
Thylachium africanum	Capparaceae	Shrub	Crater rim + Lakeshore
Vepris uguenensis	Rutaceae	Shrub	Crater rim + Savanna
Ximenia americana	Olacaceae	Shrub	Savanna
Boswellia neglecta	Burseraceae	Tree	Crater rim
Ficus sycomorus	Moraceae	Tree	Lakeshore
Acacia gerrardii	Leguminosae	Tree	Savanna
Lepisanthes senegalensis	Sapindaceae	Tree	Lakeshore
Sideroxylon sp.	Sapotaceae	Tree	Lakeshore

987

988 **Table 2**
989 Output of linear mixed-effect models for average chain length (ACL), carbon preference index (CPI),
990 the ratio of n-alkane carbon chain lengths $C_{31}/(C_{29}+C_{31})$, abundance-weighted mean hydrogen-isotopic
991 signature of C_{29} and C_{31} n-alkanes (δ^2H_{wax}), the hydrogen-isotopic signature of leaf water (δ^2H_{leaf}), and
992 biosynthetic enrichment (ε_{bio}) between δ^2H_{leaf} and δ^2H_{wax} as target variables, and with growth form (grass,
993 shrub, tree), habitat (crater rim, lakeshore, savanna) and season (long dry, NE monsoon, SE monsoon,
994 short dry) as fixed effects and species as random effect. The reference treatment were grasses at the crater
995 rim during the long dry season.

Regression coefficients		ACL	CPI	$C_{31}/(C_{29}+C_{31})$	δ^2H_{wax}	δ^2H_{leaf}	ε_{bio}
Intercept		30.8	21.7	0.76	-153	-5	-147
R^2	Fixed effects	0.18	0.29	0.19	0.40	0.08	0.19
	Random effects	0.61	0.33	0.47	0.39	0.61	0.63
	Overall model	0.79	0.61	0.66	0.80	0.69	0.83
Fixed effect parameter estimates		**ACL**	**CPI**	$C_{31}/(C_{29}+C_{31})$	δ^2H_{wax}	δ^2H_{leaf}	ε_{bio}
Growth form	Shrub	-1.0	-11.2	-0.31	36	0	38
	Tree	-0.6	-6.6	-0.18	43	7	38
Habitat	Lakeshore	0.3	-0.1	0.05	7	4	1
	Savanna	0.2	0.6	0.02	-11	3	-15
Season	NE monsoon	-0.1	3.3	0.02	-8	6	-13
	SE monsoon	0.1	-2.3	0.03	-9	-4	-9
	Short dry	-0.2	-0.2	-0.03	0	9	-12

996